Liu *et al. Chem Synth* 2022;2:21
DOI: 10.20517/cs.2022.26

Chemical Synthesis

Review

Open Access

Fundamentals of the catalytic conversion of methanol to hydrocarbons

Zhaohui Liu, Jianfeng Huang*

State Key Laboratory of Coal Mine Disaster Dynamics and Control, Institute of Advanced Interdisciplinary Studies, School of Chemistry and Chemical Engineering, Chongqing University, Chongqing 400044, China.

***Correspondence to:** Prof. Jianfeng Huang, State Key Laboratory of Coal Mine Disaster Dynamics and Control, Institute of Advanced Interdisciplinary Studies, School of Chemistry and Chemical Engineering, Chongqing University, Chongqing 400044, China. E-mail: jianfeng.huang@cqu.edu.cn

How to cite this article: Liu Z, Huang J. Fundamentals of the catalytic conversion of methanol to hydrocarbons. *Chem Synth* 2022;2:21. https://dx.doi.org/10.20517/cs.2022.26

Received: 12 Sep 2022 **First Decision:** 4 Nov 2022 **Revised:** 19 Nov 2022 **Accepted:** 25 Nov 2022 **Published:** 6 Dec 2022

Academic Editor: Ying Wan **Copy Editor:** Peng-Juan Wen **Production Editor:** Peng-Juan Wen

Abstract

For more than four decades, the methanol-to-hydrocarbons (MTH) reaction has been a successful route to producing valuable fuels and chemicals from non-petroleum feedstocks. This review provides the most comprehensive summary to date of recent research concerning the mechanistic fundamentals of this important reaction, covering different reaction stages. Mechanisms that have been proposed to explain the initial C-C bond formation during the induction stage of the MTH reaction are introduced, including the methoxymethyl cation, Koch carbonylation, carbene and methane-formaldehyde processes. At present, there is no consensus regarding these hypothetical mechanisms as a consequence of the limited amount of conclusive experimental evidence. The steady state of the MTH reaction is also examined with a focus on the widely accepted indirect hydrocarbon pool mechanism and the dual cycle concept that provides a mechanistic basis for the effects of zeolite structures and reaction conditions on product distribution. In the following section, advanced characterization techniques capable of providing new insights into the formation of coke species during the MTH reaction and innovative approaches effectively inhibiting coke formation are introduced. Finally, a summary is provided and perspectives on current challenges and the future development of this area are presented.

Keywords: Methanol to hydrocarbons, zeolite, reaction mechanism, C-C bond formation, product selectivity, catalyst deactivation

INTRODUCTION

The methanol-to-hydrocarbons (MTH) reaction catalyzed by zeolites was first discovered by Mobil scientists in 1977[1] and subsequently commercialized for the first time in New Zealand in 1985[2]. This process then became an important platform for the production of various high-demand chemical commodities, such as via methanol to gasoline (MTG)[3,4], methanol to olefins (MTO)[5-9], methanol to propene (MTP)[10-12] and methanol to aromatics (MTA) systems[13-15]. Since the MTH reaction uses methanol or dimethyl ether (DME) as the feedstock, both of which can be readily produced from nonpetrochemical resources such as natural gas, coal and biomass[16-18], this process provides an alternative to current petroleum-based synthetic routes and has thus attracted extensive attention[19-21].

In addition to obvious economic benefits[22,23], understanding the complex MTH reaction mechanism as a means of improving efficiency represents an important fundamental research goal. Over the past several decades, numerous studies of MTH have been reported and various reaction mechanisms have been proposed. There have also been several review articles in the literature that focus on different aspects of the MTH reaction, including the effects of zeolite pores on product selectivity[4,22], the sub-reactions associated with the dual cycle mechanism[20], the analysis of chemical kinetics using molecular modeling[24] and principles for the design of catalysts[21].

This review aims to provide a comprehensive summary of the MTH reaction mechanisms reported to date. To this end, the mechanisms associated with the different reaction stages are separately elucidated. We first discuss four direct mechanisms explaining the formation of the first C-C bond during the induction period. These comprise the methoxymethyl cation, Koch carbonylation, carbene and methane-formaldehyde mechanisms. These discussions primarily focus on the differences between the proposed mechanisms as well as areas where there is a lack of consensus. Advances in characterization techniques that have provided new experimental evidence and an improved understanding of these long-standing issues are also assessed. The next section examines the MTH process when in the steady state, which primarily determines product selectivity, with a focus on the widely accepted indirect hydrocarbon pool mechanism and the dual cycle concept. On the basis of the well-developed dual cycle mechanism, the effects of zeolite structures and reaction conditions on product distribution are explained. In particular, the enhanced production of propene based on optimizing the extent to which the aromatic and olefin cycles proceed is discussed. Subsequently, the deactivation of MTH catalysts is assessed. This section presents the most recent works investigating the mechanisms by which coke species [comprising primarily polycyclic aromatic hydrocarbons (PAHs) and oxygen-containing species] are formed and introduces some effective approaches to reducing coke formation. Finally, we conclude this review with a summary and share our vision for the future of MTH research.

FORMATION OF THE INITIAL C-C BOND

Since the 1970s, numerous scientists have devoted considerable effort to determining the mechanism of the MTH reaction and more than twenty different theories have been proposed. However, the precise route to the formation of the first C-C during the induction stage of the MTH reaction is still being debated. Initially, it was believed that trace impurities (potentially originating from the methanol feed, incomplete combustion of organics in the zeolite, the carrier gas or other sources) were responsible for the conversion of methanol in any direct mechanism that converts methanol/DME to hydrocarbons via a coupling process[25]. This concept was dominant for a long time, primarily because of a lack of convincing experimental data to support a direct mechanism. More recently, there has been much research devoted to the analysis of the first C-C bond formed in the initial reaction stage. Several years ago, Yarulina *et al.* and Olsbye *et al.* discussed potential mechanisms in high-quality reviews[21,26]. The present review provides more

recent discoveries based on the use of advanced characterization techniques, with a particular focus on elaborating on the reasons for the ongoing lack of consensus. Four firmly supported direct mechanisms are discussed in this section.

Methoxymethyl cation mechanism

In 2003, Wang *et al.* found that methanol or DME molecules are adsorbed on Brønsted acid sites to produce surface methoxy species (SMSs) that are highly active with regard to hydrocarbon generation[27]. This prior work indicated that, rather than organic impurities affecting product distribution or the hydrocarbon pool species, these SMS sites could promote the initial C-C bond formation during the MTH reaction[28]. With the ongoing development of spectroscopic techniques, many investigations of the first C-C bond formation have been performed and the facile generation of SMSs as active intermediates on catalytic sites has often been confirmed. As an example, Li *et al.* observed the formation of methoxy groups on the zeolite SAPO-34 using infrared (IR) spectroscopy and proposed that methoxymethyl cations ($CH_3OCH_2^+$) generated by the reaction of SMSs with DME served as intermediates[29]. These cations are coupled with additional DME/methanol molecules to produce various compounds incorporating C-C bonds (such as 1,2-dimethoxyethane and 2-methoxyethanol)[29]. In 2017, Wu *et al.* successfully observed a surface metheneoxy analog species on ZSM-5 with the aid of a solid-state nuclear magnetic resonance (NMR) technique and hypothesized that the strong interaction of the active C-H bond in DME/methanol adsorbed on the zeolite with SMSs played a crucial role in the initial C-C bond formation process[30]. In 2018, Wang *et al.* observed the bonding of SMSs to extra-framework Al atoms on ZSM-5 using ^{13}C-{^{27}Al} solid-state NMR, thus establishing the possibility of interactions between these Al atoms and SMSs[31]. In addition, SMSs adsorbed on the 8-MR pore windows of the zeolite SAPO-34 were detected by Lo *et al.* using synchrotron X-ray powder diffraction-mass spectrometry (MS) with Rietveld refinement of the data[32]. This prior work demonstrated that the presence of SMSs limited the diffusion of C_4 species through the pore openings of the SAPO-34 and thus facilitated the production of light olefins during the MTO reaction[32]. More recently, Sun *et al.* reported the first observation of surface ethoxy species serving as ethene precursor on a CHA zeolite during an MTH reaction using *in situ* solid-state NMR[33]. Ab initio molecular dynamics simulations were also applied to simulate the dynamics of the first C-C bond generation. As shown in Figure 1, the presence of a reactive SMS intermediate on an active site was determined by NMR analysis and a short-range collision between a DME molecule and this SMS was found to activate the DME. Subsequently, the first C-C bond was formed via an electrophilic attack to produce a C_2 precursor[33]. These previous studies confirmed the formation of methoxymethyl cations as a consequence of the reactions between SMSs and methanol/DME, representing the methoxymethyl cation mechanism.

Koch carbonylation mechanism

The electrophilic C in methanol/DME and the nucleophilic C in CO readily undergo an addition reaction to form a C-C bond. In 2016, Liu *et al.* proposed that the carbonylation of SMSs contributes to the first C-C bond formation to generate an acetyl species that then dissociates to produce methyl acetate or acetic acid, which can be detected as intermediates [Figure 2][34]. While monitoring the MTH reaction over ZSM-5 at 400 °C, this same group detected an increased conversion rate following the addition of CO to the methanol feedstock. Since here the involved carbonylation is similar to the Koch-type carbonylation by which carboxylic acids can be produced from the reaction of high-pressure CO with alcohols/olefins and H_2O, the mechanism for the C-C bond formation was recognized as the Koch carbonylation mechanism. The feasibility of the Koch carbonylation mechanism has also been supported by theoretical calculations that have shown a relatively low energy barrier of 80 kJmol^{-1} compared with the value of 330 kJmol^{-1} for the ylide-type mechanism[34,35]. Using solid-state NMR and operando UV-visible diffuse reflectance spectroscopy, Chowdhury *et al.* identified a direct C-C bond-containing species, i.e., surface-bound acetate, a known Koch carbonylation product that can be obtained from SMSs[36]. The surface-bound acetate species

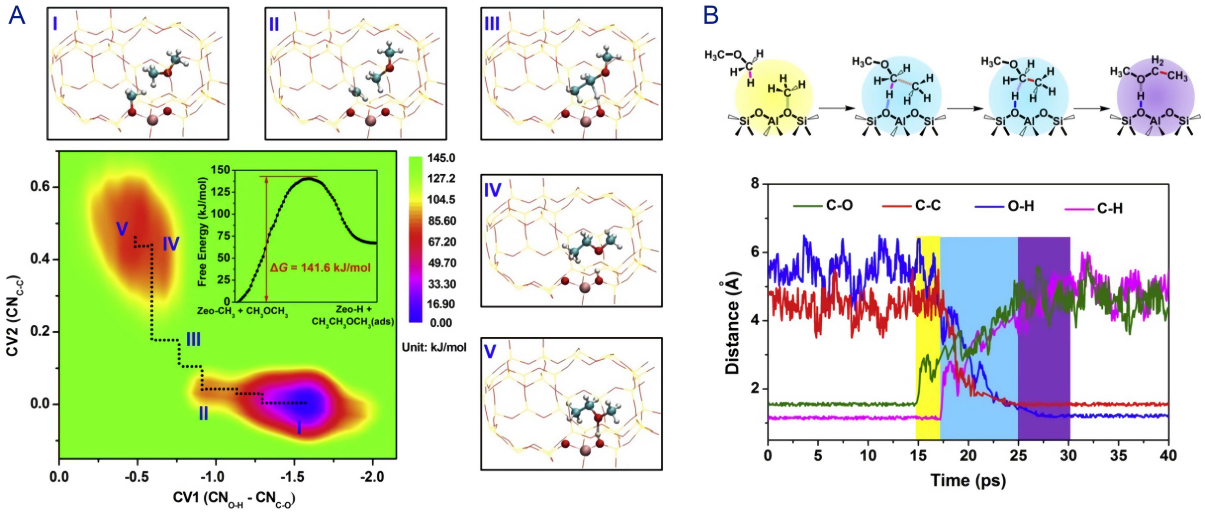

Figure 1. An ab initio molecular dynamics simulation of C-C bond formation subsequent to the collision of DME with an SMS. (A) The two-dimensional free energy surface and minimal energy path associated with the first C-C bond formation. The images show five (meta-) stable states: (I) reactant basin, (II) approaching state, (III) activation state, (IV) product state and (V) product basin. (B) Changes in the C-O, C-C, O-H and C-H bond distances in DME and the SMS over the SSZ-13 zeolite. Reproduced with permission from ref. 33[33]. Copyright 2021, Elsevier. DME: Dimethyl ether; SMS: surface methoxy specie.

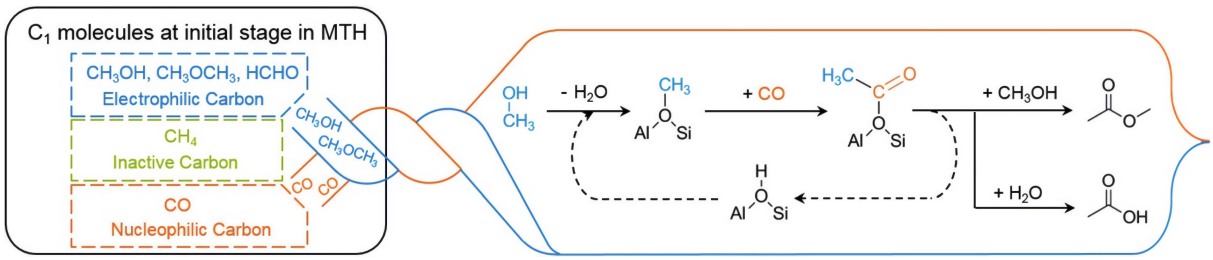

Figure 2. A diagram showing the initial C-C bond formation via the Koch carbonylation mechanism. Reproduced with permission from ref. 34[34]. Copyright 2016, Wiley-VCH. MTH: Methanol-to-hydrocarbons.

reacted with methanol to produce methyl acetate, as confirmed by the ^{13}C NMR signals at 55.2 and 178.5 ppm[36]. Very recently, using *in situ* Fourier transform IR spectroscopy, Airi *et al.* tracked the roto-vibrational CO signal throughout a methanol conversion reaction over the catalyst CoAlPO-18 and the resulting data provided support for a Koch carbonylation process involving SMSs and CO[37]. Plessow *et al.* also provided theoretical evidence for the Koch carbonylation mechanism using a model in which CO was formed from the dehydrogenation of methanol via a formaldehyde intermediate[38]. In 2019, Yang *et al.* confirmed the formation of acetaldehyde as a result of the reaction of SMSs, CO and H_2 based on a combination of online MS and NMR spectroscopy[39]. In addition, using the advanced operando synchrotron photoelectron-photoion coincidence technique, Wu *et al.* observed the production of a ketene from methyl acetate, further confirming the occurrence of carbonylation during the MTH reaction[40].

Carbene mechanism

In addition to reacting with cations (such as methoxymethyl cation) and CO, SMSs can also serve as methylation agents via the formation of carbene-like species. In 2008, Wang *et al.* reported that the C-H bonds of SMSs can be activated at high reaction temperatures to generate active compounds possessing carbene/ylide-like properties[41]. Indirect evidence for this phenomenon was also obtained from a carbene trapping experiment in which cyclohexane was used as the probe molecule and a typical carbene insertion

reaction generated a methylcyclohexane indicator[41]. Following this early work, Yamazaki *et al.* obtained direct evidence of a carbene-like intermediate using IR spectroscopy. Monitoring the IR spectra of samples obtained during the reaction of surface-bound deuterated methoxy (OCD_3) with ethene at 250 °C over ZSM-5 indicated that the intensities of the C-D stretching bands decreased while a peak related to an acidic O-D group appeared at 2655 cm^{-1} and increased in intensity, demonstrating the attachment of a D atom to a neighboring O[42]. Additional evidence for this process was obtained by reacting OCD_3 with DME at 200 °C[43]. In 2016, Chowdhury *et al.* provided further support for the carbene mechanism on the basis of analyses by two-dimensional magic angle spinning ^1H-^{13}C and ^{13}C-^{13}C solid-state NMR spectroscopy[36]. As shown in Figure 3A and B, the peaks at 57.7 ppm in the ^{13}C NMR spectrum and at 3.54 ppm in the ^1H NMR spectrum were assigned to SMSs and the strong cross-peak between ^{13}C NMR signals revealed the proximity of the SMSs to adsorbed methanol molecules. The close proximity of the 57.7 and 52.2 ppm peaks in the ^{13}C NMR spectrum was attributed to interactions of the polarized C-H bonds in the SMSs with neighboring O atoms [Figure 3C]. This result indicated the insertion of carbenes into the sp^3 C-H bonds of methanol molecules. Dimethoxymethane and its hydrolysis product methanediol were also detected in this prior work [Figure 3D and E][36]. More recently, Minova *et al.* employed Fourier transform IR spectroscopy with a mass spectrometer to directly observe the deprotonation of SMSs in large single crystals of SAPO-34[44]. This process was thought to initiate the first C-C bond formation via the insertion of a carbene into an adjacent methoxy group[44].

Methane-formaldehyde mechanism

In 1984, Kubelková *et al.* demonstrated the formation of formaldehyde and methane as a result of methanol disproportionation on ZSM-5 at 400 °C, working at low methanol pressures[45]. In 1987, Hutchings *et al.* observed the formation of methane prior to C_{2+} hydrocarbons in conjunction with low methanol coverage of the catalyst[46]. Based on these findings, the methane-formaldehyde mechanism has been postulated as yet another theory regarding the initial C-C bond formation process during the MTH reaction[46,47]. In this mechanism, methanol and SMS first react to produce formaldehyde and methane, after which the C-C coupling of the formaldehyde with a CH_3^- anion generated by the donation of an H^+ cation from CH_4 to ZO^- (i.e., deprotonated zeolite) occurs to produce ethanol [Figure 4][26]. Several recent studies using advanced analytical techniques have also confirmed the formation of methane and formaldehyde. As an example, Liu *et al.* identified the formation of olefins following the reaction of CH_4, HCHO and CO using *in situ* IR spectroscopy in conjunction with MS[48]. Wen *et al.* employed *in situ* synchrotron radiation photoionization MS to quantify the amount of formaldehyde generated during the reaction[49]. Data such as these provide solid evidence to support the methane-formaldehyde mechanism.

HYDROCARBON POOL MECHANISM AND THE DUAL CYCLE CONCEPT

An autocatalytic process occurring during the induction stage of the MTH reaction and related to the direct mechanisms has attracted much attention from researchers. Several excellent reviews have fully summarized the development of these mechanisms[21,26]. Although a general agreement has been reached regarding the formation of the initial C-C bond via a direct mechanism involving the direct coupling of methanol with its derivatives (e.g., methoxymethyl cations, CO, carbene, formaldehyde), the exact mechanistic process for each direct mechanism has not yet been fully established. Moreover, computational results have shown that the energy barrier to the direct coupling mechanism is very high and the reaction intermediates are labile, making direct C-C bond formation difficult to achieve[35,50]. While there are ongoing debates regarding the initial C-C bond formation mechanism, an indirect hydrocarbon pool mechanism which is responsible for the later stages after the initial C-C bond formation in MTH reactions has now been widely accepted with abundant supporting evidences.

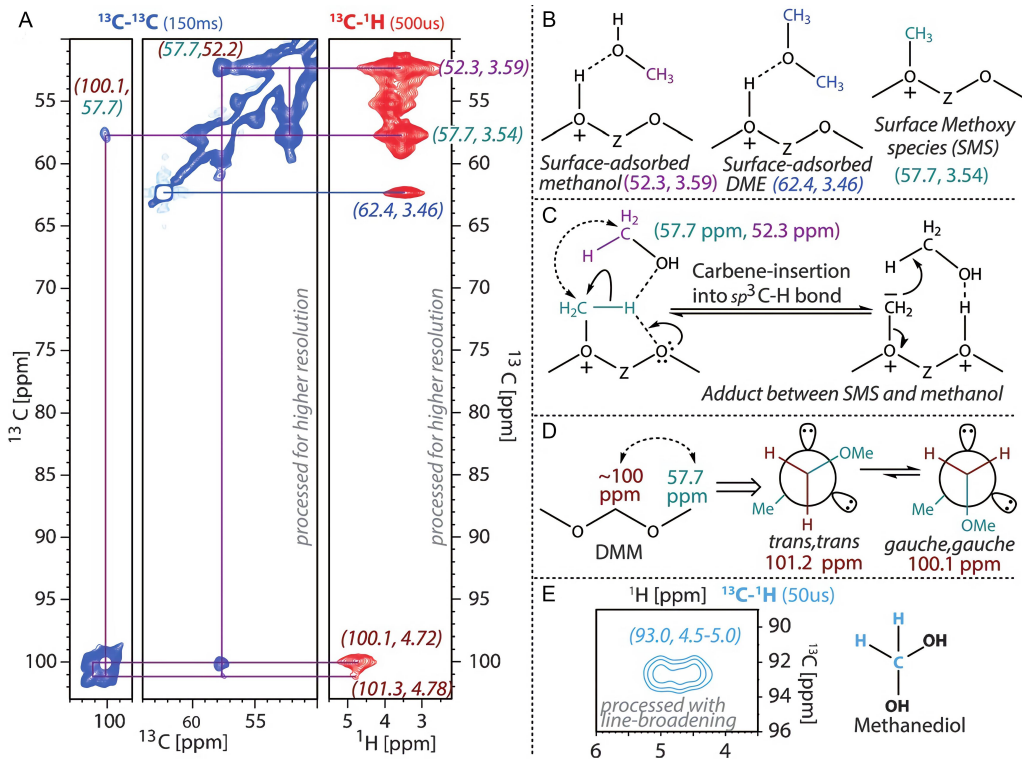

Figure 3. NMR spectra of methanol, SMSs and acetal species on SAPO-34. (A) Magnifications of two-dimensional ^{13}C-^{13}C (blue) and ^{13}C-^{1}H (red) solid-state NMR spectra acquired with a mixing time of 150 ms and a cross-polarization contact time of 500 µs. (B) Structures associated with peaks related to different surface species including methanol, DME and SMSs. (C) Identification of a surface adduct between an SMS and methanol (solid arrows: electron flows, dotted arrows: ^{13}C-^{13}C NMR correlation). (D) Chemical exchange of anomeric conformations of DMM as evident from the ^{13}C-^{13}C NMR data. (E) Identification of methanediol from the ^{13}C-^{1}H NMR data with a cross-polarization contact time of 50 µs. Reproduced with permission from ref. 36[36]. Copyright 2016, Wiley-VCH. NMR: Nuclear magnetic resonance; DME: dimethyl ether; SMSs: surface methoxy species.

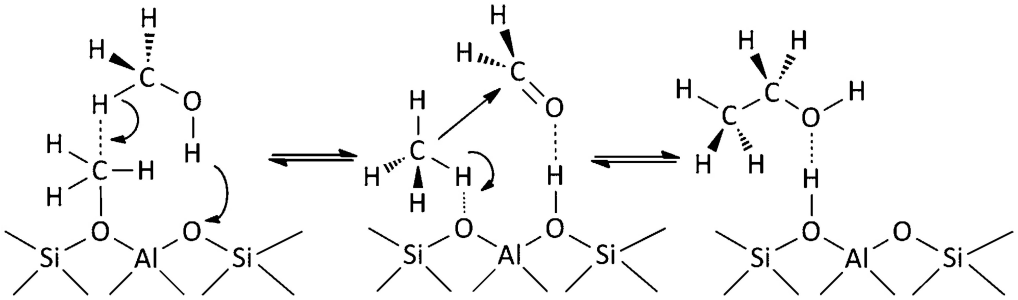

Figure 4. A diagram summarizing the methane-formaldehyde mechanism. Reproduced with permission from ref. 26[26]. Copyright 2015, Royal Society of Chemistry.

The proposed hydrocarbon pool mechanism and the dual cycle concept

In the 1990s, Dahl *et al.* first proposed the hydrocarbon pool mechanism for the MTH reaction[51,52]. In this process [Figure 5A], methanol molecules first generate a pool of hydrocarbon species [$(CH_2)_n$]. These species are active and further react with the reactant methanol to generate multiple products, including olefins, alkanes and aromatics. Simultaneously, coke is produced from the hydrocarbon pool species[52]. This indirect hydrocarbon pool mechanism has been widely studied and the associated theory has evolved considerably over time. In 2000, Song *et al.* found that the use of pretreated SAPO-34 containing

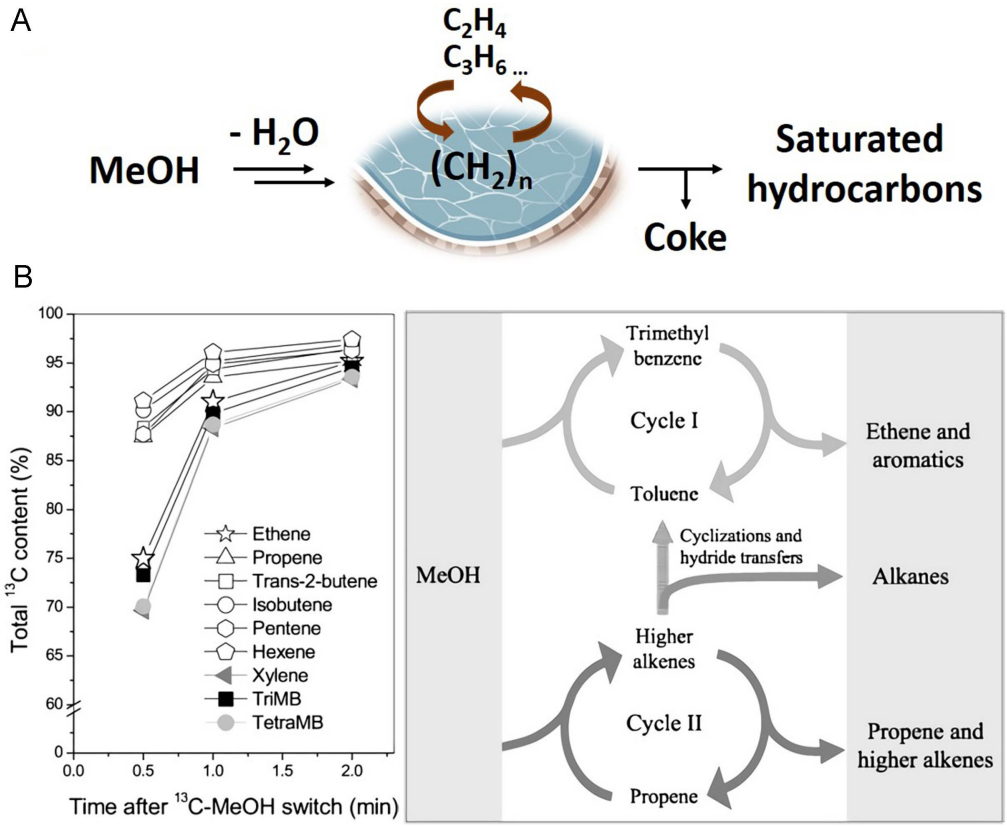

Figure 5. (A) The hydrocarbon pool mechanism for MTH conversion. Adapted with permission from ref. 52[52]. Copyright 1996, Elsevier. (B) The total ^{13}C concentrations in the reaction products (left) and the proposed dual cycle concept for the MTH reaction on ZSM-5 (right). Reproduced with permission from ref. 55[55]. Copyright 2007, Elsevier. MTH: Methanol-to-hydrocarbons.

methylbenzenes greatly increased the extent of methanol conversion from just 14% in the case of fresh catalyst to approximately 100%, suggesting that methylbenzenes were the active intermediates in the hydrocarbon pool[5]. Based on the co-reaction of ^{13}C-methanol with ^{12}C-benzene, which yields methylbenzenes, in a beta zeolite, Bjørgen *et al.* demonstrated the insertion of ^{12}C atoms in both the reaction effluent and identified the compounds retained in the catalyst, providing concrete evidence for the active nature of methylbenzenes[53].

Another important theory that evolved from the hydrocarbon pool mechanism is the dual cycle concept. Isotopic switching experiments in which a ^{12}C-methanol feedstock was switched to ^{13}C-methanol during the steady state of the MTH process by Bjorgen *et al.* indicated that the amount of ^{13}C inserted into ethene closely matched that in the methylbenzenes while the amounts of ^{13}C in propene and higher olefins were highly similar [Figure 5B][54,55]. These results demonstrated that there were two different groups of active intermediates in the MTH hydrocarbon pool, leading to the dual cycle concept. In this mechanism, aromatic intermediates and olefins simultaneously react to generate complex products, representing a modification of the hydrocarbon pool mechanism[54,55]. Notably, this isotopic switching technique is commonly accepted and widely applied to the study of dual cycle reaction routes.

Elementary reactions

The proposed dual cycle mechanism has made a significant contribution to our understanding of the effect of the hydrocarbon pool on product selectivity. However, many different elementary reactions comprise the

overall MTH process and an assessment of the kinetics of the pool species and the associated sub-reactions can help to elucidate links between the dual cycle mechanism and various products. In this regard, Ilias *et al.* produced an excellent review focusing on the chemistry of the MTH reaction[20]. Here, we provide a brief introduction to the sub-reactions and primarily concentrate on the effects of these sub-reactions on product distribution. Based on the dual cycle mechanism, six important elementary reactions may be associated with the MTH process, as discussed in the following paragraphs.

Olefin methylation, generating higher olefins by incorporating methyl groups into light olefins, is the main way for the C-C chain growth in MTH reactions. A prior kinetic study established that such reactions are primarily affected by the olefin pressure with only a minimal effect from methanol/DME[56-61], on the basis of the relationship between olefin methylation rate and the partial pressure of reactants (i.e., light olefin and methanol/DME) which implies that, during this process, the active sites on the catalyst are fully saturated by methyl groups obtained from methanol or DME[20]. Additionally, with increases in olefin size, the activation energy barrier decreases and the methylation rate increases, such that highly branched aliphatic compounds are favored as intermediates during MTH conversion[56-61]. Interestingly, the oligomerization of light olefins is also an effective source of the C-C chain growth of hydrocarbons and can be catalyzed by the Brønsted acid sites of zeolites. Similar to the olefin methylation reaction, the formation of heavy olefins via this route is promoted by moderate temperatures and high pressures[62,63].

Olefin cracking was first reported by Dessau and LaPierre[64,65] and was proposed as an important means of increasing the yield of propene in Lurgi's MTP reaction on ZSM-5[20]. During this process, alkoxides formed by the protonation of long-chain olefins generate short-chain olefins and small alkoxides through β-scission. The small alkoxides subsequently desorb from the catalyst and acquire protons. The competition between methylation and cracking is a critical factor that decides the resulting product distribution. Specifically, more rapid olefin cracking tends to produce lower molecular weight olefins, while a slower reaction gives higher molecular weight olefins that eventually generate aromatics via cyclization reactions. The rates of β-scission also affect the proportion of olefins in the product mixture[66-68]. Simonetti *et al.* found that the rate of C_5 methylation was more than 100 times that of β-scission, but the C_8 olefin (i.e., 3,4,4-trimethyl-2-pentene) had a higher rate of β-scission[66]. Buchanan *et al.* also revealed that the olefin cracking process was enhanced by elongating the olefin chains[68].

Hydrogen transfer and cyclization reactions can function as bridges between olefin- and aromatic-based cycles in MTH reactions. Higher olefins tend to produce aromatic compounds via hydrogen transfer together with the formation of stoichiometric amounts of alkanes. This process can be quantified using the hydrogen transfer index[69-72]. Specifically, this index can be used as an indicator for the formation of aromatics and the participation extent of the associated catalytic cycle (i.e., aromatic-based cycle)[73]. It should also be noted that cycloalkanes and cycloolefins are unstable products that quickly dehydrogenate to produce aromatics, so the cyclization process also contributes to the propagation of the aromatic cycle. Fan *et al.* found that dienes and monoenes can also form methylcyclohexenes via the Diels-Alder reaction based on assessments using solid-state NMR and gas chromatography (GC)-MS[74]. The same group also demonstrated that the Diels-Alder process exhibited much lower energy barriers than the oligomerization and cyclization reactions along the route to the construction of large molecules[74].

The methylation of aromatics is similar to that of olefins, but the dealkylation of the former can follow two different routes: the paring and side-chain mechanisms [Figure 6][75]. These two mechanisms both begin with the gem-methylation of methylbenzene. In the former, this step results in a ring contraction to generate a five-membered ring with an alkyl substituent that can produce either ethene or propene via

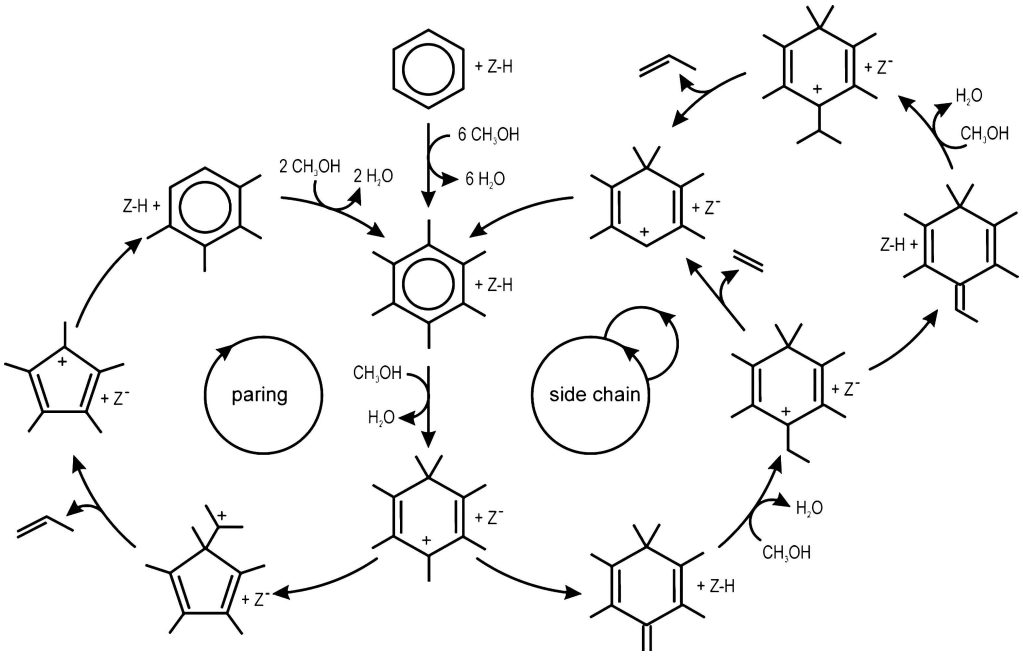

Figure 6. A diagram summarizing the paring and side-chain mechanisms. Reproduced with permission from ref. 75[75]. Copyright 2009, Wiley-VCH.

dealkylation[76-78]. The participation of cyclopentenyl cations in this mechanism has previously been confirmed by IR and NMR analyses[77-79]. In the case of the side-chain mechanism, following the release of a proton, an exocyclic double bond is formed that then undergoes stepwise side chain methylation and dealkylation[75,80]. Hexamethenecyclohexadiene and a heptamethylbenzenium cation have also been identified using GC-MS and NMR, providing direct evidence for the side-chain mechanism[81].

Contribution of catalytic cycles to product formation

In-depth investigations of the dual cycle mechanism have been performed in attempts to assess the relative contributions of the two cycles to the product distribution generated by the MTH reaction. As discussed above, each catalytic cycle contains different elementary sub-reactions that will vary with the reaction conditions and catalysts employed. Careful kinetic studies of these different sub-reactions have provided much knowledge regarding the effects of these elementary steps on product distribution and the dominant catalytic cycle.

Hill *et al.* recently carried out a detailed study of the dual cycle mechanism[59-61,82]. They first systematically investigated the rate constants for ethene and propene methylation over four zeolites (MFI, BEA, MOR and FER) and found that propene methylation had higher rate constants (by an order of magnitude) and lower activation energies compared with ethene methylation[59]. On the basis of isotopic switching experiments that showed that ethene was a product of the aromatic dealkylation process[55], this group proposed that ethene was an end product and could be used as an indicator of the progression of the aromatic cycle. Similarly, because alkanes formed during the MTH reaction are inactive, these compounds can serve as indicators of the occurrence of the olefin catalytic cycle. However, alkanes are also formed via a hydrogen transfer process that is related to aromatic formation. To exclude this effect, the same group proposed that the total yield of 2-methylbutane and 2-methyl-2-butene could serve as an indicator of the progression of the olefin-based cycle, while the ethylene/(2-methylbutane + 2-methyl-2-butene) ratio could be used to assess the extent to which aromatic-/olefin-based cycles occurred during the MTH reaction over ZSM-5[82].

Building on Bhan's work, Sun *et al.* suggested slightly different indicators for the dual cycles[83,84]. In the case of the aromatic-based cycle, they concluded that methane can also be formed via the dealkylation of methylbenzene and represents a terminal product of this catalytic cycle, meaning that the formation of this compound should exhibit the same trend as ethene. In contrast, the selectivity for C_4-C_7 aliphatics, which readily diffuse out of ZSM-5, can be employed as an indicator for the olefin-based cycle[83,84]. It is known that propene can be produced in both catalytic cycles and is also able to react with methanol as an olefin intermediate. Another important feature of the dual cycle mechanism is that the two catalytic cycles compete for acidic sites. Based on such fundamental information concerning the dual-cycle mechanism, researchers are trying many different approaches to achieving the selective propagation of one specific cycle as a means of obtaining product selectivity from the MTH reaction[20,82,83].

PRODUCT SELECTIVITY

The product distribution obtained from the MTH reaction during its steady state is an important aspect of the process and has therefore been extensively studied. Many factors, including the raw material feed, reaction conditions and zeolite structure, can have significant effects on the reaction routes and subsequently on product distribution. In the following section, we elaborate on the influences of these factors on product formation during the MTH reaction with a particular focus on the effects of zeolite structure.

Active intermediates in the raw material feed

According to the dual cycle concept, increasing the relative amounts of specific active species in the feedstock should enhance certain catalytic cycles to promote the formation of desired products. As an example, the addition of toluene or p-xylene to the methanol feedstock has been found to increase the formation of methane, ethene and aromatic products while decreasing the amounts of C_4-C_7 aliphatics [Figure 7A]. These results can be attributed to promotion of the aromatic-based cycle and inhibition of the olefin catalytic cycle upon adding active aromatic compounds. Interestingly, the addition of a low concentration of C_{3-6} olefins cannot effectively restrain the aromatic-based catalytic cycle as a result of the rapid transformation of these compounds to aromatics[83]. Bhan's group also found that the addition of small amounts of acetaldehyde (1-4 C%) to the methanol stream led to a monotonic enhancement of the ethene selectivity, ranging from 9.3 C% to 15 C% in trials with bulk ZSM-5 and from 1.4 C% to 6.4 C% in trials with diffusion-free ZSM-5 nanosheets. In addition, methylbenzene selectivities from 4.9 C% to 7.8 C% with bulk ZSM-5 and from 2.6 C% to 5.3 C% with ZSM-5 nanosheets were observed. Although acetaldehyde is not a direct active hydrocarbon pool species, it can produce aromatics through a multistep aldol-condensation reaction[85]. Zhang *et al.* also recently reported a kinetics study showing that the addition of olefins (such as in the case of olefin recycling) to the feedstock enhanced the olefin methylation and cracking processes, facilitating the formation of propylene during the MTP reaction[86].

Reaction conditions

Elementary reactions have varied kinetic orders and active energies, so the reaction temperature and pressure will affect the rates of these sub-reactions differently and thus modify the product distribution. For example, Goetze *et al.* found that 1-methylnaphthalene deactivated the MTH reaction at 350 °C on the zeolite DDR but functioned as a catalytically active intermediate at 450 °C[87]. The same group established that the primary active intermediates during the MTO reaction over CHA zeolites varied at different temperatures. Specifically, methylbenzenes were the main active species at low temperatures (300-350 °C), whereas methylated naphthalenes were the primary active intermediates at higher temperatures (350-500 °C)[88,89]. However, Qi *et al.* reported that naphthalene species can also serve as active intermediates at a lower temperature of 290 °C in trials using ZSM-5[90]. In addition, Yarulina *et al.* found that adjusting the temperature from 380 to 475 °C changed the ethene: propene ratio obtained from the MTO reaction

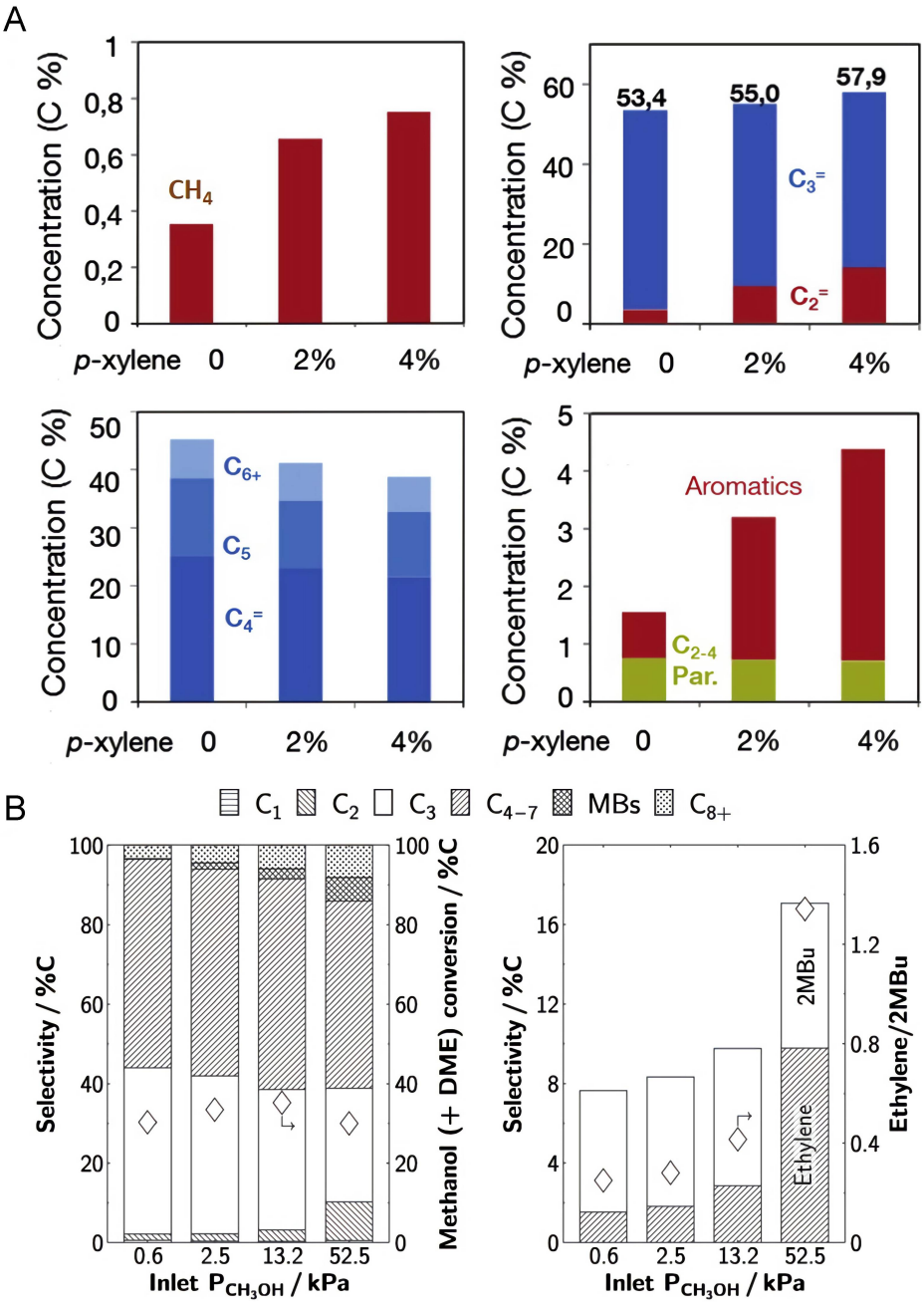

Figure 7. (A) The effect of co-feeding p-xylene on product distribution. Reproduced with permission from ref. 83[83]. Copyright 2014, Elsevier. (B) Product selectivity and methanol conversion (left), selectivities for ethene and 2-methyl-2-butene + methylbutane (right). Reproduced with permission from ref. 73[73]. Copyright 2017, Elsevier.

over a Sigma-1 zeolite from 0.5 to 1.6[91]. This same reaction gave a butene yield of 14 C% at 380 °C but yields of less than 5 C% at a higher temperature of 475 °C[91].

Arora *et al.* demonstrated the effect of the methanol partial pressure on the product distribution [Figure 7B][73]. As a typical example, increasing the methanol pressure from 0.6 to 52.5 kPa during the MTH process over ZSM-5 at 400 °C increased the selectivities for methylbenzenes and ethene from 0.1 C% to 5.9 C% and from 1.5 C% to 9.8 C%, respectively. In contrast, the propene selectivity decreased from 41.8 C%

to 28.7 C% such that the propene/ethene (P/E) ratio was decreased by a factor of 9. It was concluded that a higher methanol pressure facilitated the hydrogen transfer reaction which, in turn, generated large amounts of aromatics during the MTH reaction[73].

Zeolite structure

As a result of the rapid development of crystalline zeolites with ordered micropores having sizes in the range of 0.3-1 nm, such materials have been widely used as catalysts or sorbents. These inorganic substances include aluminosilicates, aluminophosphates and silicates, and the International Zeolite Association database currently contains over 200 different types of zeolites. Their topologies (based on the presence of cavities and channels), morphologies (that is, the crystal dimensions and mesoporosities) and compositions (the relative amounts of Si, Al, P, Ti and other elements) of these materials vary greatly and all these factors can affect catalytic performance in the MTH reaction.

The first factor assessed herein is topology. As an example, ZSM-22 has one-dimensional 10-MR channels that are too narrow to allow the formation of methylbenzene intermediates, thus inhibiting the aromatic catalytic cycle but promoting the olefin-based cycle to produce a high proportion of branched C_{5+} paraffins[92,93]. The ZSM-5 zeolite, which has an MFI structure containing three-dimensional 10-MR pores approximately 5.6 Å in size, produces a mixture of olefins, paraffins and aromatics, while the small-pore CHA-structured SAPO-34 containing pore opening of only approximately 3.8 Å mainly produces C_2-C_4 alkenes under similar reaction conditions[19]. Moreover, the primary active hydrocarbons during the MTH reaction over zeolites also vary in morphology. Hexa- and penta-methylbenzenes were found to be the main active hydrocarbon pool intermediates in trials using a beta zeolite, facilitating the production of propene and butenes[53]. In contrast, the reaction intermediates were restricted to xylenes and tri-methylbenzenes in work with ZSM-5, which produced ethene and propene[54].

The texture of the zeolite is another important factor determining the MTH reaction mechanism. In particular, the transport of reactants and products across the channels in the zeolite plays a vital role[94]. A Fickian diffusion model in which the zeolite is assumed to be a spherical crystal without any other transport restrictions can be used to calculate the adsorption properties of a zeolite under isothermal conditions[95,96]. This method allows a quantitative comparison of the difference between zeolite sizes, which can have a remarkable effect on product selectivity during the MTH reaction[97,98]. Studies have shown that increasing the ZSM-5 particle size increases the selectivity for ethene while reducing that for C_4-C_7 aliphatics. The same trend in product selectivity was also observed in trials in which access to ZSM-5@SiO_2 was blocked by the formation of a SiO_2 shell. These results show that a large effective crystallite size prolongs the residence time of large active methylbenzenes in the catalyst particles, facilitating the aromatic-based cycle to produce light olefins[97]. Work with the self-pillared pentasil ZSM-5 having a diffusion length of only 1 nm indicated that the ethene selectivity resulting solely from olefin interconversion was limited to 1.1% because the aromatic cycle essentially did not proceed in the zeolite[98]. The effects of using a mesoporous beta zeolite as the catalyst in the MTH reaction were previously examined. The results indicated that intracrystalline mesoporosity provided much shorter diffusion lengths than those in the standard material, leading to better catalytic performance in terms of conversion capacity, reaction rate and lifetime. More importantly, methylbenzenes could easily diffuse out of the mesoporous catalyst so that less ethylene but more long-chain aliphatics were obtained compared with the conventional beta zeolite[99].

In addition to the diffusion effect, the product distribution is also sensitive to the acidity of the zeolite. In 2011, Wei *et al.* reported that ZSM-5 zeolites with different SiO_2/Al_2O_3 ratios all showed high MTH activity, but the propene selectivity was 45.9% greater on a Na-ZSM-5 specimen having a high SiO_2/Al_2O_3 ratio of

220[100]. In 2017, Zhao *et al.* achieved an elevated propene selectivity of 58.3% using a high-Si structured beta zeolite-catalyzed MTP process because the olefin-based catalytic cycle was the dominant reaction route[101]. In 2018, Yarulina *et al.* determined that ZSM-5 modified with alkaline earth metals had a lower density of Brønsted acidic sites[102]. This suppressed the accumulation of aromatics but allowed the olefin methylation/cracking process to proceed, leading to the generation of more propene and less ethene than were obtained using pure ZSM-5[102]. In cooperation with Bhan's group, the authors also investigated the effects of the SiO_2/Al_2O_3 ratio in ZSM-5 zeolites on the formation of ethene during DME conversion. This work indicated that a high aluminum content increased the interactions between aromatics and catalytic sites before these compounds exited the crystalline particles, providing higher selectivity for ethene. As noted above, increasing the catalyst particle size can also increase the interactions between aromatics and catalytic sites by prolonging the residence time of the methylbenzenes. These two factors were therefore combined to produce a single descriptor (N_{H+}) for ethene selectivity. Increasing the N_{H+} value was found to promote both catalytic cycles, although the aromatic cycle was promoted to a larger extent than the olefin cycle, meaning that ethene formation was enhanced[103]. Very recently, Liang *et al.* proposed that the relationship between the acid site density and the aromatic-based cycle is more complicated than is presently thought[104]. Isotopic tracing experiments by this group showed that the acid site density had a negligible impact on the reactivity of active aromatics that were preferentially transformed into coke precursors and thus caused deactivation of the catalytic sites[104]. Moreover, Yuan *et al.* showed that active Al atoms located on the external surfaces of ZSM-11 promoted rapid coke formation, while the uniformly distributed Al species in the micropores inhibited the aromatic-based cycle during the MTO reaction[105].

Zeolites having small pores tend to exhibit high selectivity for light olefins because they are able to confine larger organic compounds produced during the MTO reaction. The MTO process is an important reaction in C1 chemistry and is capable of producing valuable olefin-based chemicals via non-petroleum routes. Many fundamental investigations of this process have also recently been performed. Initially, aromatic-based species were widely believed to function as active intermediates during the MTO reaction because of the shape-selective effect of the small pores in the catalysts. Isotopic studies have also demonstrated that methylbenzenes make the main contribution to the production of olefins[106]. Analyses by GC-MS and solid-state NMR have produced evidence for the presence of active hexamethenecyclohexadiene and the heptamethylbenzenium cation[81]. In addition, operando UV-visible spectra have indicated that methylated aromatic species are the major active species[88,89]. However, variations in the specific aromatic compounds in the hydrocarbon pool can have a significant effect on the MTO products. Kang *et al.* systematically established the correlations between the cage sizes of small-pore zeolites and the MTO product distribution[107]. This work compared 30 different zeolites having 14 different cage-type topologies and found that the MTO reaction proceeded in a similar manner on specific topologies independent of the composition[107]. As shown in Figure 8, an ellipsoidal model was initially defined based on three axes, with *ab* denoting the cage-defining ring and *b* being the ring size. As the ellipsoidal cage size was increased from 12-ring to 16-ring, the primary light olefin product changed from ethene to butene, so a relationship between ring size and product selectivity could be established. These results suggest that the ellipsoidal cages in small-pore zeolites determine the sizes of methylated aromatic intermediates during the MTO process[107].

In addition to aromatic active species, olefin-based catalytic intermediates formed during the MTO process are also of interest. Based on an analysis of ^{1}H and ^{13}C NMR spectra, Dai *et al.* identified several olefin-like species in trials using SAPO-34 during the induction period of the MTO reaction, and suggested that these compounds evolved into aromatic intermediates when the reaction was in the steady state[8]. However, the functioning of these olefin-like species as active intermediates was not assessed[8]. Hwang *et al.* showed that active olefin intermediates appeared during the MTO reaction in an early stage but also established that

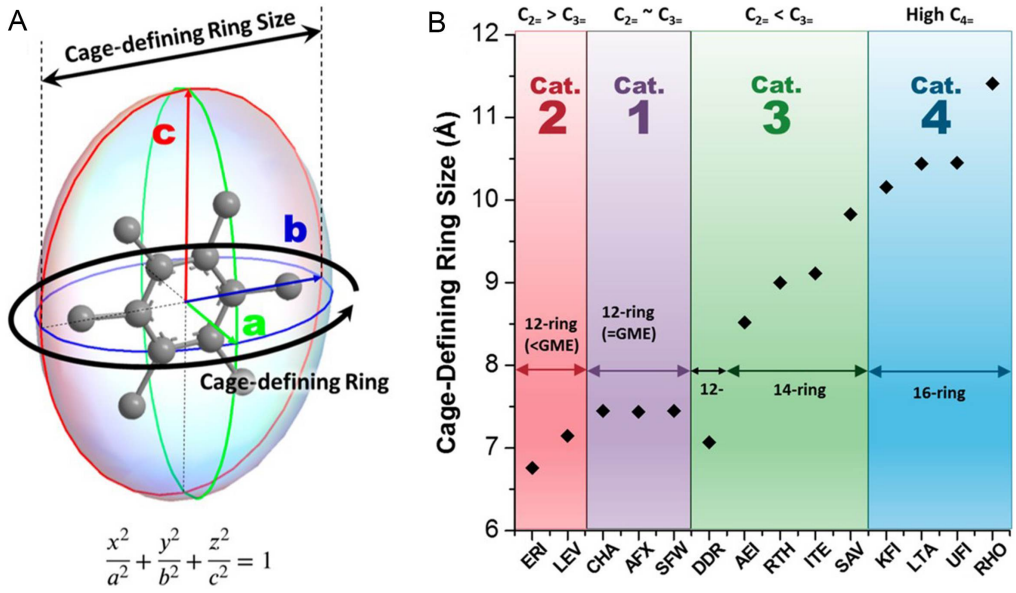

Figure 8. (A) The ellipsoidal model of a cage-defining ring. (B) Correlations between cage-defining ring sizes and olefin distributions. Reproduced with permission from ref. 107[107]. Copyright 2019, American Chemical Society.

accumulated aromatics dominated the catalytic process and increased the turnover number[108]. More recently, the authors found that propene selectivity underwent a monotonic increase with decreases in the aluminum content or crystal size of DDR zeolites[109]. As shown in Figure 9A, $^{12}C/^{13}C$ methanol switch results indicated that the formation of propene was closely associated with the propagation of the olefin-based cycle, an effect that has been neglected in most studies. The authors have proposed that catalytic behavior during this process is related to the presence of small pores in the zeolite that restrict the diffusion of both aromatics and long-chain olefin intermediates. The effect of olefin-related β-scission reactions during the entire process was also determined to be significant[109]. Yang *et al.* prepared a SAPO-14 zeolite with ultrasmall cages (5.3 × 10.05 Å) and an AFN topology and reported 77.3% propene selectivity from a one-pass methanol conversion process with a time-on-stream of 3 min, representing the highest value up to that point [Figure 9B][110]. Using $^{12}C/^{13}C$-methanol switch experiments, the same group established that the olefin-based route, rather than a mechanism based on aromatics, dominated the conversion of methanol [Figure 9C] and thus maximized the selectivity for propene based on the effect of limited diffusion[110]. Zhou *et al.* fabricated a SAPO-14 zeolite with a high Si content and achieved a P/E ratio of 4.17 during the MTO reaction at 450 °C[111]. These studies served to fill gaps in the body of knowledge regarding the effect of the olefin-based cycle on MTO reactions.

MTP reaction

Ethene, propene and aromatics are the main value-added products that can be obtained from the MTH process. The dual cycle mechanism indicates that the formation of ethene and aromatics is largely associated with the aromatic-based cycle, while the production of propene is connected with either the olefin-based or aromatic-based cycles. Because of the complexity of the MTH reaction network, adjusting the single-pass selectivity for propene to achieve a high selectivity value is highly desirable. Based on the preceding discussions of the reaction mechanism, effective means of enhancing the propene yield are discussed below.

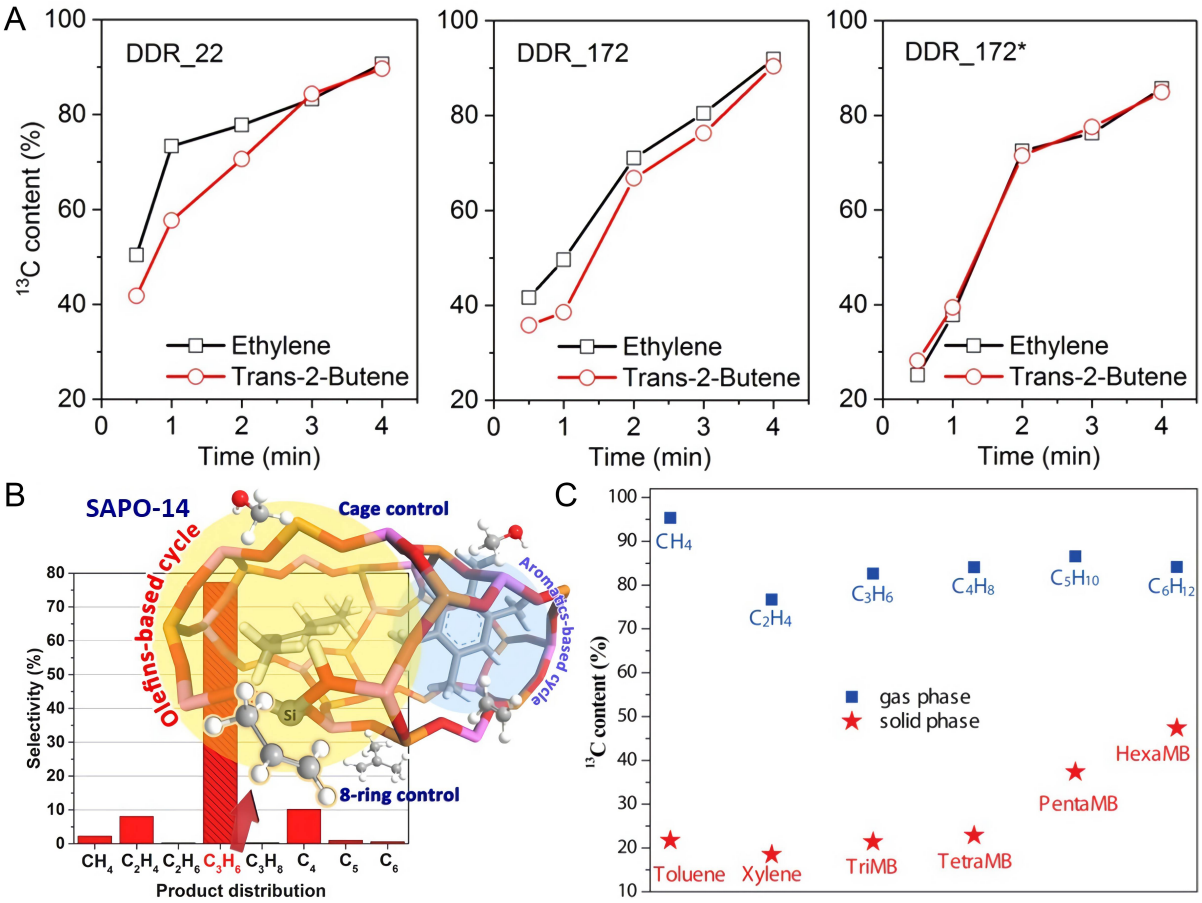

Figure 9. (A) The ^{13}C concentrations in ethene and trans-2-butene over time during ^{12}C/^{13}C-methanol switch experiments using various DDR zeolites. Reproduced with permission from ref. 109[109]. Copyright 2020, American Chemical Society. (B) Product distribution and (C) ^{13}C concentrations in effluents and residual methylbenzenes during the MTO reaction over SAPO-14. Reproduced with permission from ref. 110[110]. Copyright 2020, American Chemical Society. MTO: Methanol to olefins.

In general, the MTH process can take place only in the cages and interconnected channels of zeolites. Therefore, the structures of zeolites have a substantial effect on the catalytic route and affect the final product selectivity. Dyballa *et al.* compared three different 10-MR zeolites having varying structures (ZSM-5, ZSM-11 and ZSM-22) in MTP reactions and demonstrated that propene selectivity, coke formation and catalyst lifetime were highly dependent on the acid density of the material[112]. As indicated by the data in Table 1, a propene selectivity greater than 50% could be achieved over ZSM-5 (130) (here, the number 130 in the bracket indicates the Si/Al ratio of the zeolite) and ZSM-11 (200). Moreover, regardless of the morphology, the propene selectivity and the P/E ratio increased with increasing Si/Al ratio[112]. Adding a binder[113] and heteroatoms such as B[114], Mn[12] and Ca[102] had a similar effect to that of increasing the Si/Al ratio to dilute the acid density, and greatly enhanced propene selectivity. This phenomenon was especially noticeable in trials using the catalysts B-CON[115] (with a propene selectivity of 60%) and Mn-ZSM-5 (200)[12] (with a propene selectivity of 58.4%). This research showed that decreasing the density of Brønsted acid sites hindered the hydrogen transfer process and changed the main catalytic route during the MTH process. As a result, the olefin-based cycle became dominant, leading to a high propene selectivity.

Hierarchically structured zeolites (also referred to as mesoporous zeolites) combine the advantages of micropores and mesopores to provide an enhanced molecular diffusion rate. As discussed above in Section

Table 1. Propene selectivities over different zeolites

Catalyst[a]	Temperature (℃)	Conversion (%)	Propene Sel. (C%)	Ethene Sel. (C%)	P/E ratio	Refs. (year)
ZSM-5 (20)	450	100	27	15	1.8	[112] (2016)
ZSM-5 (130)	450	100	51	5	10.2	[112] (2016)
ZSM-11 (30)	450	94	14	10	1.4	[112] (2016)
ZSM-11 (200)	450	100	51	3	17	[112] (2016)
ZSM-22 (30)	450	100	43	9	4.8	[112] (2016)
ZSM-22 (50)	450	100	45	8	5.6	[112] (2016)
Binder-ZSM-5 (40)	450	100	41.9	5.2	8	[113] (2010)
B-ZSM-5 (162)	460	> 80	43	/	/	[114] (2014)
Mn-ZSM-5 (200)	480	100	58.4	10.6	5.5	[12] (2015)
Ca-ZSM-5 (46)	500	100	51	7.5	6.8	[102] (2018)
B-CON[b]	500	100	60	4.5	13.3	[115] (2015)
Meso-ZSM-5 (78)	470	99.6	42.2	4.18	10.1	[10] (2008)
Meso-beta (277)	550	> 99	55.5	5.6	10	[116] (2018)
2 nm ZSM-5 (87.5)	350	~50	20.5	1.5	13.7	[97] (2015)
17 μm ZSM-5 (38.0)	350	~50	26.2	20.3	1.3	[97] (2015)
100 nm ZSM-22 (46)	450	100	53	21	2.6	[117] (2014)
300 nm ZSM-22 (46)	450	100	50	21	2.4	[117] (2014)
Beta (125)	450	100	46.0	3.3	14.1	[118] (2017)
SAPO-17 (6)	425	> 98	27	55	0.5	[107] (2019)
SAPO-34 (0.123)	400	> 98	39	30	1.3	[107] (2019)
SAPO-18 (0.063)	400	> 98	46	24	1.9	[107] (2019)
DDR (22)	400	~50	38.1	36.6	1.0	[109] (2020)
DDR (172)	400	~50	48.3	27.8	1.7	[109] (2020)
Meso DDR (172)	400	~50	50.6	26.4	1.9	[109] (2020)
SAPO-14[c]	400	89.2	77.3	8.0	9.7	[110] (2020)
SAPO-14[c]	450	99.3	65.7	15.9	4.1	[110] (2020)

[a]The number in brackets is the Si/Al ratio of the zeolite. [b]Si/B = 22. [c]Al:P:Si = 0.50:0.48:0.02.

"Zeolite structure", mesoporous zeolites have very short diffusion lengths of only a few nanometers and show promise as catalysts when applied to the MTP process. As reported previously, meso-ZSM-5[10] and meso-beta[116] zeolites produce more propene than their counterparts because the short diffusion lengths in these materials favor the olefin-based cycle and limit the aggregation of aromatics[97]. However, Khare *et al.* achieved a propene selectivity of only 20.5% with 2 nm ZSM-5 (87.5) particles at 350 °C, albeit with a high P/E ratio of 13.7[97]. These results were attributed to the relatively low reaction temperature, at which the methylation and oligomerization of low alkenes proceeded rather than the cracking process that would be expected to produce light olefins. Therefore, a high temperature (typically above 400 °C)[117,118] is needed for the MTP reaction, as indicated in Table 1.

Small-pore zeolites are highly selective for both ethene and propene because the smaller openings in these catalysts easily trap large products. As the aromatic-based cycle proceeds, ethene is inevitably produced via the dealkylation of branched aromatics and subsequently competes with the formation of propene. As such, the P/E ratio is usually less than 2 [Table 1][107]. However, many groups have recently made efforts to tune the P/E ratio obtained during the MTO reaction. Kang *et al.* established that the topology of a small-pore zeolite can determine the branching of aromatics in the cages and release different olefins through dealkylation[107]. Tuning the acid content and crystallization size of small-pore zeolites is also an effective strategy to regulate the relative extents to which the two catalytic cycles proceed[109,110] and this approach has

previously been used in work with medium-/large-pore zeolites. Notably, Liu's group achieved the highest-ever propene selectivity of 77.3% using a newly developed small-pore SAPO-14 zeolite[110]. Compared with the complex outflows from medium- or large-pore zeolites, the main products of the MTO process over small-pore zeolites are limited to light olefins. As a consequence, it is easier to adjust the selectivity for propene when using small-pore zeolites. The data discussed in this paragraph therefore suggest innovative approaches to designing and engineering catalysts for the MTP process.

CATALYST DEACTIVATION

Pore blocking by polycyclic aromatic hydrocarbons

The deactivation of catalysts is another issue with equal importance to the product selectivity of the MTH reaction. As the MTH reaction proceeds over molecular sieve catalysts, many cross-linked PAHs featuring graphene-like structures are formed via the cage-passing growth of confined hydrocarbon pool species. This phenomenon suppresses mass transfer, blocks the catalytic centers and deactivates the catalyst. According to the mechanism described in Section "FORMATION OF THE FIRST C-C BOND", the MTH reaction proceeds based on a pool of hydrocarbons that produce needed light olefins but also undesirable heavy molecules that cause catalyst deactivation[119-124]. Much effort has been devoted to understanding this deactivation phenomenon. In 2020, Lezcano-Gonzalez *et al.* tracked the formation of carbonaceous species during the MTO reaction using a newly developed operando Kerr-gated Raman spectroscopic technique that discriminated between Raman signals and fluorescence[125]. This work examined the formation of heavy hydrocarbons at different stages of the MTO reaction and showed that small branched polyenes with reduced mobility [Figure 10A-C] eventually underwent a cyclization process to form PAHs within large cages [Figure 10D]. However, an MFI topology that provided steric constraint inhibited the cyclization of polyenes and thus the generation of PAHs, increasing the catalyst lifetime[125]. Using a single-crystal electron diffraction technique, Wennmacher *et al.* found that the nucleation of coke began at channel intersections while large PAHs were preferentially formed in straight pores[119].

Similar to the outcomes of many other reactions, the coke generated during the MTH process is a complex mixture of various polycyclic aromatics with broad mass distributions[126-129]. However, in the case of the MTH reaction, the deactivating species are uncertain in terms of their exact compositions and chemical structures and are largely related to the pore structure of the zeolite. For example, hexamethylbenzene is an active pool species in reactions over beta and SAPO-34 zeolites but can also function as a deactivation species in conjunction with other topologies such as ZSM-22 (with a pore size of 4.6 × 5.7 Å)[26]. Interestingly, the hydrocarbon pool species undergo spatial interactions with the zeolite framework and thus cause the zeolite cells to expand[130-132]. Yang *et al.* investigated the dynamic structural evolution of SAPO-34 induced by organic compounds using ^{27}Al and ^{31}P NMR spectroscopy[132]. The ^{31}P NMR signal was found to shift from -30.1 to -30.8 ppm with the accumulation of deposits, indicating an increase in the P-O-Al bond angle[132]. In addition to expanding the unit cells in the zeolite, coke can grow by traversing the windows of zeolitic cages to form cross-links with neighboring coked cells and therefore generate large interconnected multicore PAHs[133]. Based on analyses by matrix-assisted laser desorption ionization-Fourier transform ion cyclotron resonance (MALDI-FT-ICR) with MS and isotope labeling, Wang *et al.* developed a so-called aromatic cage-passing deactivation mechanism occurring in MTO reactions over different small-pore zeolites[133]. In these materials, aromatics with three or four rings are initially formed in the cages and then cross the opening windows and link together as the reaction proceeds. As shown in Figure 11, the chemical composition of the coke will vary with changes in the zeolite cavity shape, suggesting that the coke formation/deactivating processes in zeolite-type catalysts are also associated with a shape-selective effect similar to product selectivity[133].

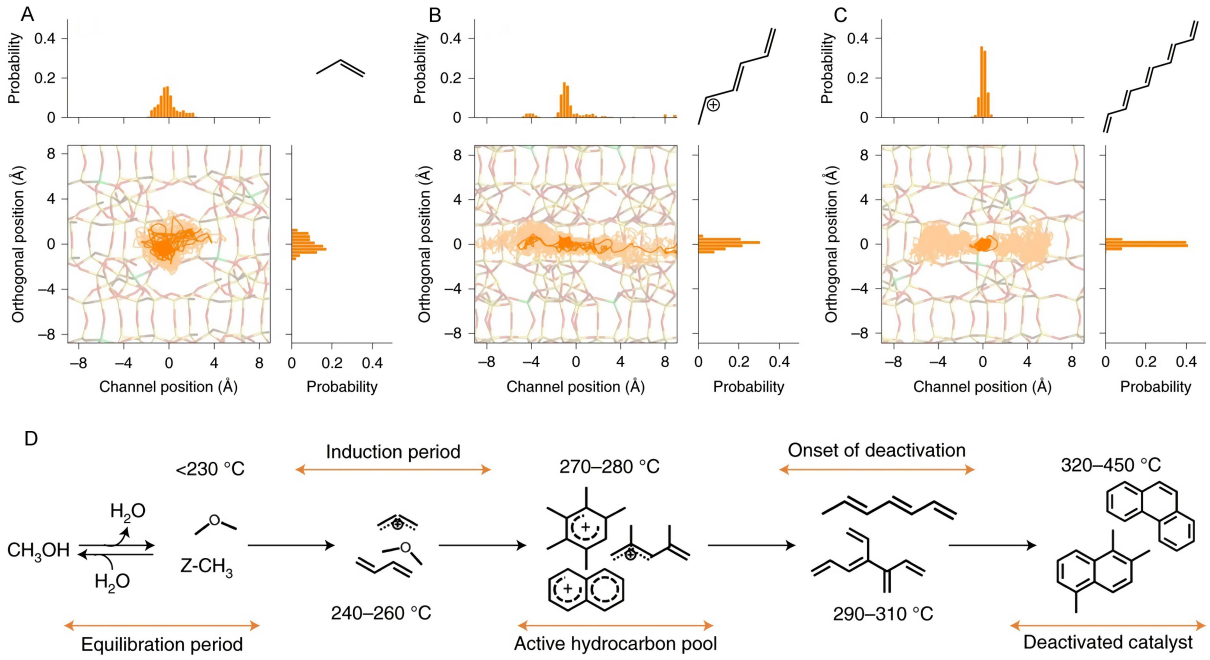

Figure 10. (A-C) The mobility of polyene species and (D) hydrocarbon species evolution during the MTO reaction. Reproduced with permission from ref. 125[125]. Copyright 2020, Nature Publishing Group. MTO: Methanol to olefins.

Conventional zeolites with ordered cavities and microporous channels can serve as molecular sieves, explaining the unique shape selectivity function within the MTH reaction. However, micropores also impose restrictions on molecular diffusion throughout the zeolite crystals. Hierarchical zeolites containing mesopores provide enhanced mass transfer and exhibit prolonged lifetimes during the MTH reaction[120,134]. Choi *et al.* prepared thin ZSM-5 nanosheets that showed reaction times five times that of bulk ZSM-5 particles as a consequence of the rapid mass diffusion and high coke tolerance of the sheets[135]. Liu *et al.* fabricated single-crystalline hierarchical ZSM-5 zeolites via a protozeolite seeding method[136]. These materials contained faceted mesopores and possessed high hydrothermal stability, exhibiting a remarkable lifetime of 18 h and an impressive propylene selectivity of up to 52.7%[136]. Using high-resolution electron energy loss spectroscopy, the authors probed the distribution of coke species in a mesoporous beta zeolite (Beta-MS) and a conventional beta zeolite (Beta-C) following the MTH reaction [Figure 12]. A significant difference observed in elemental carbon mapping data is that coke species were uniformly distributed throughout each entire Beta-MS crystal, while the coke in Beta-C crystals was mainly concentrated close to the particle exteriors [Figure 12B and E]. This same work examined the chemical compositions of carbon-based coke compounds at different locations. These analyses showed that H-rich coke with low molecular weights was deposited in the micropores but the intracrystalline mesopores in Beta-MS accommodated heavy graphite-like species [Figure 12C and F][99]. The data also suggested that micropores containing methylbenzenes and long-chain aliphatics may remain active during the MTH reaction even if the channels are blocked by large coke molecules. Liang *et al.* reported that the high density of surface acid sites on the H-MCM-22 zeolite promoted coke deposition on the external surfaces of the material[137]. In contrast, the acid sites in the sinusoidal channels in this zeolite were highly resistant to coke formation, providing additional evidence for the effects of acid site density and distribution on deactivation[137].

Oxygen-containing species promoting coke formation

In 2015, Müller *et al.* investigated the deactivation of a catalyst in a plug-flow reactor (PFR) and a fully back-mixed reactor (CSTR) and found more rapid deactivation of ZSM-5 in the PFR [Figure 13A][124]. This work

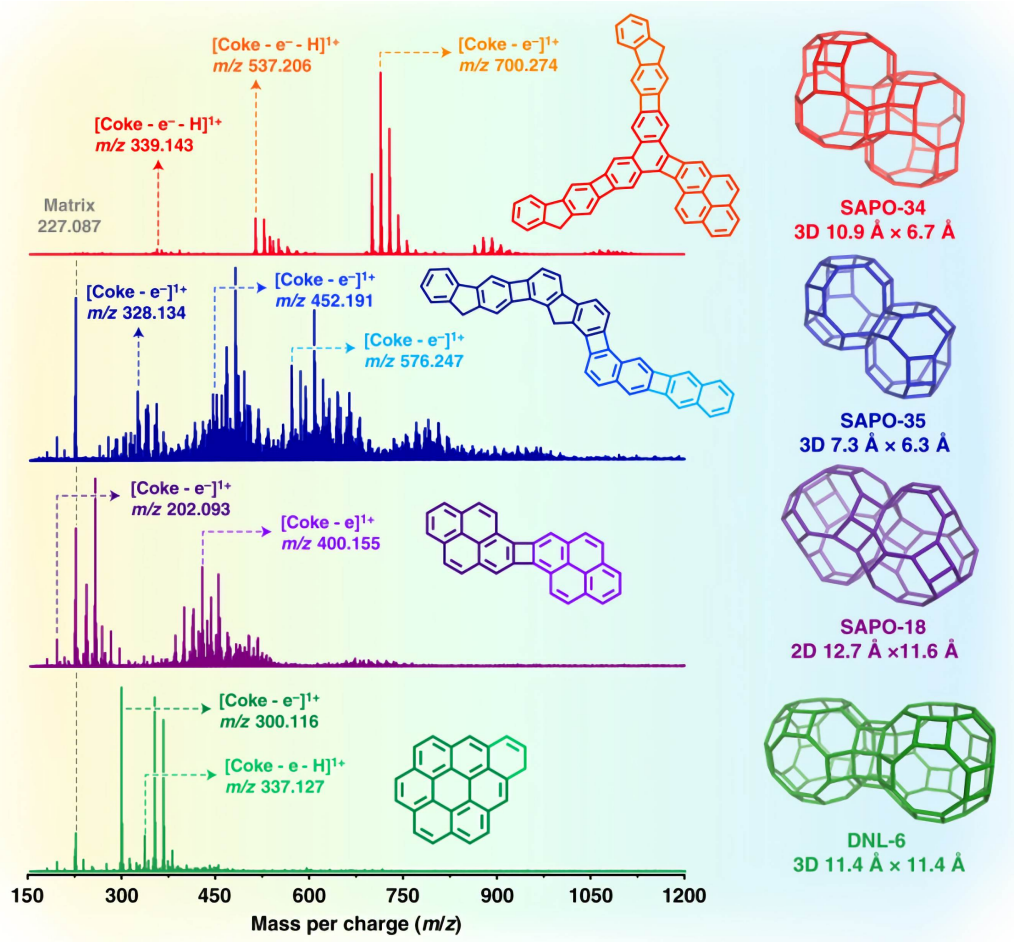

Figure 11. Molecular structures of coke species in different cage-structured zeolites and the associated MALDI FT-ICR mass spectra. Reproduced with permission from ref. 133[133]. Copyright 2020, Nature Publishing Group. MALDI FT-ICR: Matrix-assisted laser desorption ionization-Fourier transform ion cyclotron resonance.

established that the local methanol pressure in the top layer of the PFR was high, while the mixing of products with feedstock in the CSTR resulted in a more moderate methanol pressure. A mechanism was proposed to explain this phenomenon and is summarized in Figure 13B. At the start of the reaction, the relatively high methanol pressure leads to the formation of oxygen-containing compounds that strongly bind with active Brønsted acid sites on the catalyst, resulting in rapid deactivation. As the reaction continues, the O-containing surface compounds evolve into aromatics and eventually grow into typical coke molecules such as PAHs. This pioneering work established the important effect of O-containing compounds on catalyst deactivation throughout the MTH reaction[124]. In 2016, our own group observed the formation of various O-containing compounds comprising cyclopentenone derivatives during the MTH reaction by isotopic tracing with ^{13}C-methanol. As shown in Figure 13C, co-feeding this labeled compound along with the methanol feedstock showed that the presence of certain species inhibited methanol conversion by competing for adsorption on catalytic acid sites, where they were readily converted to heavy aromatics and coke species[138]. Notably, many subsequent reports following this pioneering work confirmed the appearance of the same O-containing compounds [Figure 13D][39,139].

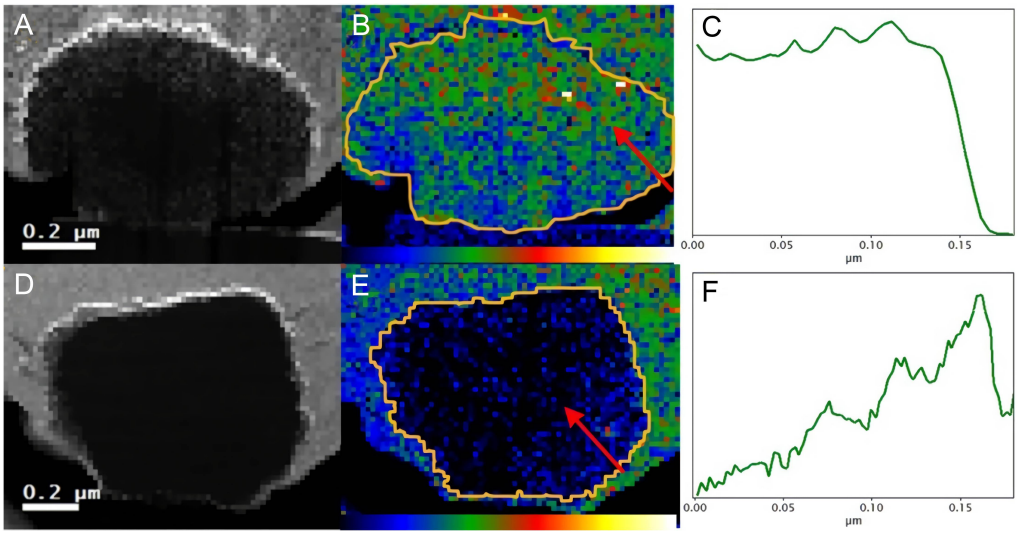

Figure 12. HAADF-STEM images (left), carbon mapping data (middle) and line profiles (right) for Beta-MS (A-C) and Beta-C (D-F). The carbon concentrations in (B) and (E) are indicated by the color bar and the red arrows show the locations at which line profiles were acquired. Reproduced with permission from ref. 99[99]. Copyright 2015, American Chemical Society.

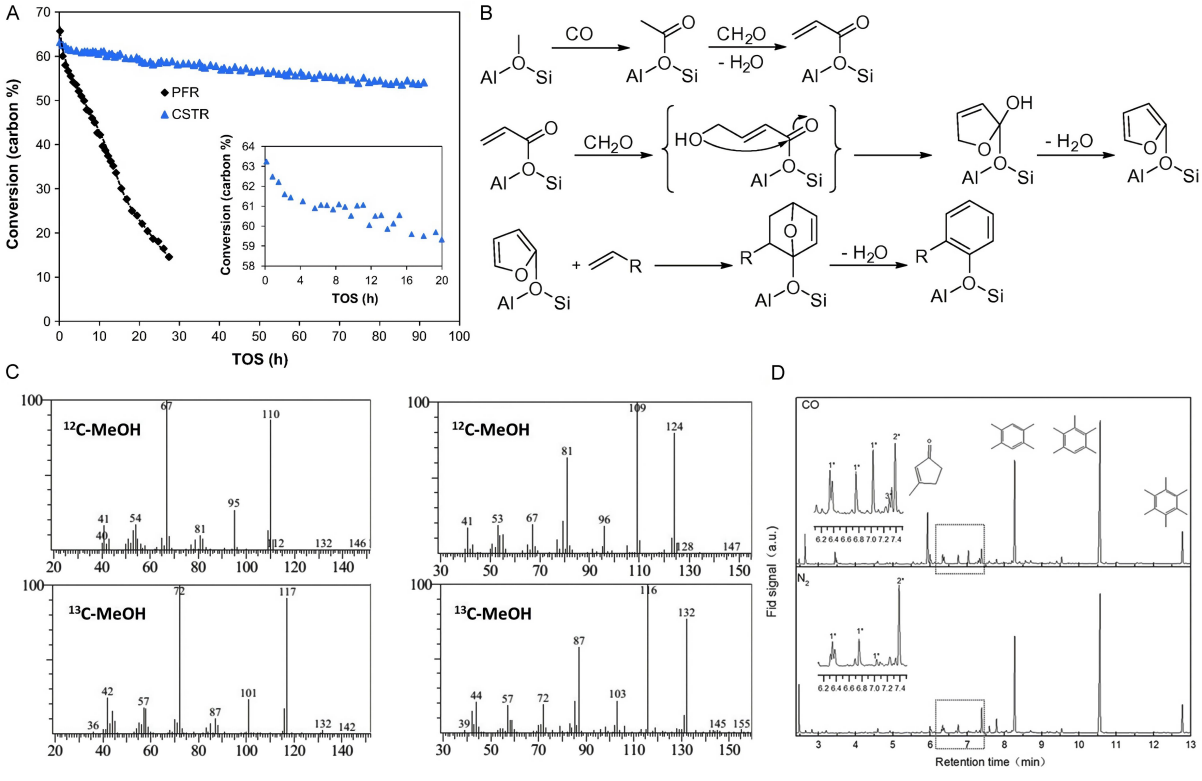

Figure 13. (A) Deactivation characteristics of a catalyst in PFR and CSTR trials and (B) proposed pathway for O-containing coke formation. Reproduced with permission from ref. 124[124]. Copyright 2015, Elsevier. (C) Mass spectra of O-containing coke compounds. Reproduced with permission from ref. 138[138]. Copyright 2016, Royal Society of Chemistry. (D) Mass spectra of organic materials retained in ZSM-5 catalysts during methanol conversion under N_2 and CO. Reproduced with permission from ref. 139[139]. Copyright 2018, Wiley-VCH. PFR: Plug-flow reactor; CSTR: continuous stirred-tank reactor.

Formaldehyde has also attracted attention as another O-containing compound that could be related to

catalyst deactivation during the MTH reaction[49,140]. Because formaldehyde readily undergoes nucleophilic addition, either the Prins or aldol-condensation reactions could produce coke precursors from this molecule[48,85]. In 2017, Martinez-espin *et al.* compared the use of methanol and DME as feedstocks for MTH reactions on ZSM-5, SSZ-24 and SAPO-5 zeolites and found that a methanol feed caused faster deactivation, which they attributed to the formation of formaldehyde[141]. More recently, Shi *et al.* reported that SSZ-13 had a shorter lifetime than SAPO-34, even though both materials have the same CHA framework[140]. The greater acid strength of the former was thought to promote the generation of formaldehyde, which subsequently transformed active intermediates into inactive polycyclic species[140,142]. This same work investigated means of circumventing formaldehyde-mediated chain carrier termination by adding Y_2O_3 to the zeolite to decompose formaldehyde[143] or combining high-pressure H_2 with the feedstock to hydrogenate the formaldehyde to methanol[144,145].

Transformation of coke to active species

Methylbenzenes, which promote the formation of light olefins in the hydrocarbon pool, can also evolve into PAHs through cyclization and cross-linking reactions. In many reactions that are known to be accompanied by coke deposition, air calcination or steam gasification is used to remove coke species as an approach to catalyst regeneration. Zhou *et al.* demonstrated that coke species confined in SAPO-34 can be directly transformed to active naphthalenic species by steam cracking, which ultimately enhances the light olefin selectivity of the process[146]. As shown in Figure 14A, increasing the treatment time applied to a coked ZEOS specimen gradually increased the concentration of naphthalene even though the total coke amount was reduced. These results suggest the stability of naphthalene under steam cracking conditions at 680 °C. More importantly, the average molecular weight of the carbonaceous species was decreased after steam treatment, indicating that H_2O could serve as an active agent to hydrogenate coke species [Figure 14B]. The Raman spectra in Figure 14C contain bands at 1360, 1415 and 1630 cm^{-1} assigned to PAHs and at 1600 cm^{-1} corresponding to the G band of amorphous carbon, all of which decreased in intensity during the early stage of steam cracking. Simultaneously, bands at 1240 and 1125 cm^{-1} assigned to branched exocyclic aromatics appeared. These results confirm that coke compounds underwent ring-opening as the catalyst was regenerated. Steam treatment has also been found to regenerate blocked micropores such that they become accessible again [Figure 14D][146]. In another study, Wang *et al.* created active naphthalenic species in SAPO-34 by ethylene pre-coking and reported that subsequent steaming of the material significantly promoted the selectivity for lower olefins and prolonged the catalyst lifetime during the MTO reaction[147].

CONCLUSION AND OUTLOOK

Over the 40-year time span during which the MTH process has been developed, this method has been recognized as an extremely important research area in the catalysis community. Several industrial plants using this process are already operated successfully, especially in China, attracting much more interest from both academia and industry. However, the fundamentals of the initial C-C bond formation mechanism are still debated. As discussed in the first part of this review, many active species have recently been discovered using advanced analytical techniques. Even so, details regarding the transformation of active species in this process remain elusive. More work is needed to investigate the mechanism responsible for the initial C-C bond formation during the MTH reaction using these advanced methods.

Understanding the mechanism of the MTH reaction and the effect of the zeolite structure will facilitate the design and synthesis of new high-performance catalysts. Based on the proposed indirect hydrocarbon pool mechanism, the direct mechanism seems unnecessary because the product distribution obtained from the MTH process can be clearly explained with the indirect mechanism, especially the dual cycle mechanism. As discussed in the second part of this review, assessments of the complexity of the catalyst compositions

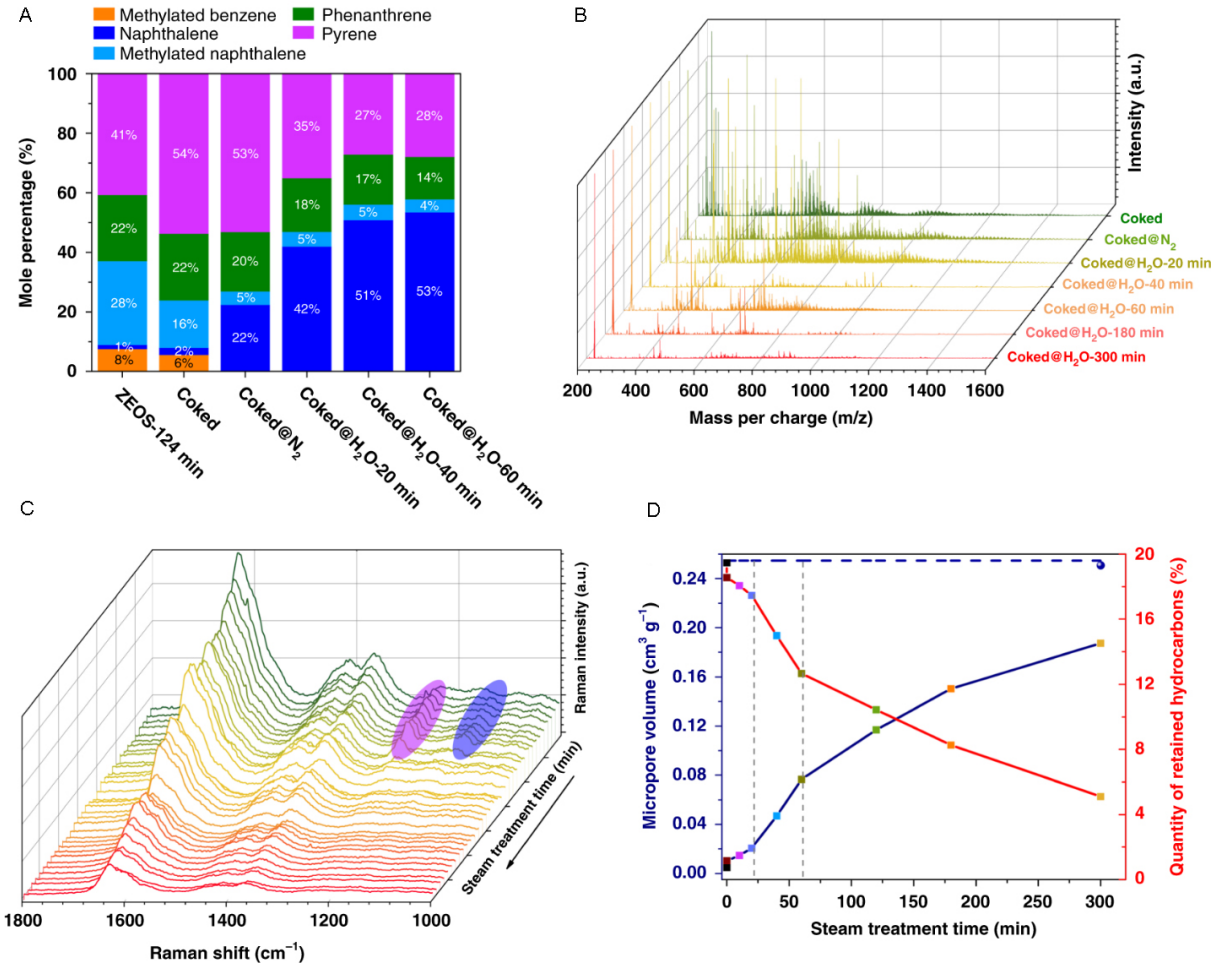

Figure 14. The formation of coke species with molecular masses (A) less than 200 Da and (B) greater than 200 Da under various conditions. (C) Operando UV-Raman spectra of a coked ZEOS specimen during steam treatment. (D) Micropore volume and coke mass of a ZEOS specimen over time during steam treatment. Reproduced with permission from ref. 146[146]. Copyright 2021, Nature Publishing Group.

and the multiple elementary sub-reactions occurring within the MTH system can provide basic knowledge that allows control of the reaction routes and product distributions. With much effort, the MTG and MTO reactions have been commercialized but not the MTP and MTA reactions. Studies of the MTP process have shown that small-pore zeolites with weak acidity show promise as catalysts for the olefin-based catalytic cycle and can increase the propene yield. The MTA process can also efficiently produce aromatics[148,149] that are very important platform molecules for high-value commodity chemicals[150]. Although the MTA reaction was not addressed in detail in this review, highly acidic zeolites having large pore channels may be able to promote this reaction based on prior research regarding the dual cycle mechanism.

Coke formation is another severe problem that cannot be avoided in the MTH reaction. Currently, the commercially available catalyst SAPO-34 is used for the MTO process with only a very short time for the one-pass reaction, after which coke deposits must be burned off by heating at high temperatures in air. This process, unfortunately, generates a considerable amount of CO_2 that is released into the atmosphere. A number of advanced techniques, such as operando Kerr-gated Raman and NMR spectroscopy, MALDI FT-ICR MS and electron energy loss spectroscopy, have provided detailed insights into the formation of coke

species. Further work, already being performed by many groups (including Olsbye, Bhan and Lercher), is required to find effective protocols to slow coke formation as a prerequisite for industrial applications.

Ever-increasing CO_2 emissions have resulted in many environmental challenges and the catalytic conversion of CO_2 to produce valuable fuels and chemicals, such as via CO_2 hydrogenation to methanol, has become one of the most effective approaches to addressing this issue. Commercial CO_2-to-renewable-methanol plants have been established in China, Iceland, Japan and elsewhere[151]. Considering the well-developed methanol-to-hydrocarbon technologies that are available, the catalytic hydrogenation of CO_2 to C_{2+} chemicals (such as olefins and aromatics) via methanol-mediated routes is especially desirable because these compounds possess higher energy densities and greater value than C_1 products[152-154]. It is our hope that this review will inspire new research intended to mitigate existing challenges associated with CO_2 hydrogenation and methanol conversion.

DECLARATIONS

Authors' contributions

Manuscript preparation and correction: Liu Z, Huang J

Availability of data and materials

Not applicable.

Financial support and sponsorship

This work was supported by the Fundamental Research Funds for the Central Universities (2020CDJQY-A072), the Venture and Innovation Support Program for Chongqing Overseas Returnees (cx2020107), the Thousand Talents Program for Distinguished Young Scholars, Natural Science Foundation of Chongqing (cstc2021jcyj-msxmX0945), and the Postdoctoral Science Foundation of China (2021M700579).

Conflicts of interest

Both authors declared that there are no conflicts of interest.

Ethical approval and consent to participate

Not applicable.

Consent for publication

Not applicable.

REFERENCES

1. Chang C. The conversion of methanol and other O-compounds to hydrocarbons over zeolite catalysts. *J Catal* 1977;47:249-59. DOI
2. Yurchak S. Development of Mobil's fixed-bed methanul-to-gasoline (MTG) process. Methane Conversion, Proceedings of a Symposium on the Production of Fuels and Chemicals from Natural Gas. Elsevier; 1988. p. 251-72. DOI
3. Lunsford JH. Catalytic conversion of methane to more useful chemicals and fuels: a challenge for the 21st century. *Catal Today* 2000;63:165-74. DOI
4. Olsbye U, Svelle S, Bjørgen M, et al. Conversion of methanol to hydrocarbons: how zeolite cavity and pore size controls product selectivity. *Angew Chem Int Ed Engl* 2012;51:5810-31. DOI PubMed
5. Song W, Haw JF, Nicholas JB, Heneghan CS. Methylbenzenes are the organic reaction centers for methanol-to-olefin catalysis on HSAPO-34. *J Am Chem Soc* 2000;122:10726-7. DOI
6. Wang C, Wang Y, Du Y, Yang G, Xie Z. Similarities and differences between aromatic-based and olefin-based cycles in H-SAPO-34 and H-SSZ-13 for methanol-to-olefins conversion: insights from energetic span model. *Catal Sci Technol* 2015;5:4354-64. DOI

7. Wang Y, Chen S, Gao Y, et al. Enhanced methanol to olefin catalysis by physical mixtures of SAPO-34 molecular sieve and MgO. *ACS Catal* 2017;7:5572-84. DOI
8. Dai W, Wang C, Dyballa M, et al. Understanding the early stages of the methanol-to-olefin conversion on H-SAPO-34. *ACS Catal* 2015;5:317-26. DOI
9. Deimund MA, Harrison L, Lunn JD, et al. Effect of heteroatom concentration in SSZ-13 on the methanol-to-olefins reaction. *ACS Catal* 2016;6:542-50. DOI
10. Mei C, Wen P, Liu Z, et al. Selective production of propylene from methanol: mesoporosity development in high silica HZSM-5. *J Catal* 2008;258:243-9. DOI
11. Firoozi M, Baghalha M, Asadi M. The effect of micro and nano particle sizes of H-ZSM-5 on the selectivity of MTP reaction. *Catal Commun* 2009;10:1582-5. DOI
12. Rostamizadeh M, Taeb A. Highly selective Me-ZSM-5 catalyst for methanol to propylene (MTP). *J Ind Eng Chem* 2015;27:297-306. DOI
13. Ni Y, Sun A, Wu X, et al. The preparation of nano-sized H[Zn, Al]ZSM-5 zeolite and its application in the aromatization of methanol. *Microporous Mesoporous Mater* 2011;143:435-42. DOI
14. Williams CL, Chang C, Do P, et al. Cycloaddition of biomass-derived furans for catalytic production of renewable p-Xylene. *ACS Catal* 2012;2:935-9. DOI
15. Zhang J, Qian W, Kong C, Wei F. Increasing para-Xylene selectivity in making aromatics from methanol with a surface-modified Zn/P/ZSM-5 catalyst. *ACS Catal* 2015;5:2982-8. DOI
16. Olah GA. Beyond oil and gas: the methanol economy. *Angew Chem Int Ed Engl* 2005;44:2636-9. DOI PubMed
17. Usman M, Daud WMAW. Recent advances in the methanol synthesis via methane reforming processes. *RSC Adv* 2015;5:21945-72. DOI PubMed PMC
18. Lebarbier VM, Dagle RA, Kovarik L, Lizarazo-adarme JA, King DL, Palo DR. Synthesis of methanol and dimethyl ether from syngas over Pd/ZnO/Al_2O_3 catalysts. *Catal Sci Technol* 2012;2:2116. DOI
19. Haw JF, Song W, Marcus DM, Nicholas JB. The mechanism of methanol to hydrocarbon catalysis. *Acc Chem Res* 2003;36:317-26. DOI PubMed
20. Ilias S, Bhan A. Mechanism of the catalytic conversion of methanol to hydrocarbons. *ACS Catal* 2013;3:18-31. DOI
21. Yarulina I, Chowdhury AD, Meirer F, Weckhuysen BM, Gascon J. Recent trends and fundamental insights in the methanol-to-hydrocarbons process. *Nat Catal* 2018;1:398-411. DOI
22. Zhong J, Han J, Wei Y, Liu Z. Catalysts and shape selective catalysis in the methanol-to-olefin (MTO) reaction. *J Catal* 2021;396:23-31. DOI
23. Tian P, Wei Y, Ye M, Liu Z. Methanol to olefins (MTO): from fundamentals to commercialization. *ACS Catal* 2015;5:1922-38. DOI
24. Speybroeck V, De Wispelaere K, Van der Mynsbrugge J, Vandichel M, Hemelsoet K, Waroquier M. First principle chemical kinetics in zeolites: the methanol-to-olefin process as a case study. *Chem Soc Rev* 2014;43:7326-57. DOI PubMed
25. Song W, Marcus DM, Fu H, Ehresmann JO, Haw JF. An oft-studied reaction that may never have been: direct catalytic conversion of methanol or dimethyl ether to hydrocarbons on the solid acids HZSM-5 or HSAPO-34. *J Am Chem Soc* 2002;124:3844-5. DOI PubMed
26. Olsbye U, Svelle S, Lillerud KP, et al. The formation and degradation of active species during methanol conversion over protonated zeotype catalysts. *Chem Soc Rev* 2015;44:7155-76. DOI PubMed
27. Wang W, Buchholz A, Seiler M, Hunger M. Evidence for an initiation of the methanol-to-olefin process by reactive surface methoxy groups on acidic zeolite catalysts. *J Am Chem Soc* 2003;125:15260-7. DOI PubMed
28. Jiang Y, Wang W, Reddymarthala V, Huang J, Sulikowski B, Hunger M. Effect of organic impurities on the hydrocarbon formation via the decomposition of surface methoxy groups on acidic zeolite catalysts. *J Catal* 2006;238:21-7. DOI
29. Li J, Wei Z, Chen Y, et al. A route to form initial hydrocarbon pool species in methanol conversion to olefins over zeolites. *JJ Catal* 2014;317:277-83. DOI
30. Wu X, Xu S, Zhang W, et al. Direct mechanism of the first carbon-carbon bond formation in the methanol-to-hydrocarbons process. *Angew Chem Int Ed Engl* 2017;56:9039-43. DOI PubMed
31. Wang C, Chu Y, Xu J, et al. Extra-framework aluminum-assisted initial C-C bond formation in methanol-to-olefins conversion on zeolite H-ZSM-5. *Angew Chem Int Ed Engl* 2018;57:10197-201. DOI PubMed
32. Lo B, Ye L, Chang G, et al. Dynamic modification of pore opening of SAPO-34 by adsorbed surface methoxy species during induction of catalytic methanol-to-olefins reactions. *Appl Catal B: Environ* 2018;237:245-50. DOI
33. Sun T, Chen W, Xu S, et al. The first carbon-carbon bond formation mechanism in methanol-to-hydrocarbons process over chabazite zeolite. *Chem* 2021;7:2415-28. DOI
34. Liu Y, Müller S, Berger D, et al. Formation mechanism of the first carbon-carbon bond and the first olefin in the methanol conversion into hydrocarbons. *Angew Chem Int Ed Engl* 2016;55:5723-6. DOI PubMed
35. Blaszkowski SR, van Santen RA. Theoretical study of C-C bond formation in the methanol-to-gasoline process. *J Am Chem Soc* 1997;119:5020-7. DOI
36. Chowdhury AD, Houben K, Whiting GT, et al. Initial carbon-carbon bond formation during the early stages of the methanol-to-olefin process proven by zeolite-trapped acetate and methyl acetate. *Angew Chem Int Ed Engl* 2016;55:15840-5. DOI PubMed PMC
37. Airi A, Damin A, Xie J, Olsbye U, Bordiga S. Catalyst sites and active species in the early stages of MTO conversion over cobalt

AlPO-18 followed by IR spectroscopy. *Catal Sci Technol* 2022;12:2775-92. DOI

38. Plessow PN, Studt F. Unraveling the mechanism of the initiation reaction of the methanol to olefins process using ab initio and DFT calculations. *ACS Catal* 2017;7:7987-94. DOI
39. Yang L, Yan T, Wang C, et al. Role of acetaldehyde in the roadmap from initial carbon-carbon bonds to hydrocarbons during methanol conversion. *ACS Catal* 2019;9:6491-501. DOI
40. Wu X, Zhang Z, Pan Z, Zhou X, Bodi A, Hemberger P. Ketenes in the induction of the methanol-to-olefins process. *Angew Chem Int Ed Engl* 2022;61:e202207777. DOI PubMed
41. Wang W, Hunger M. Reactivity of surface alkoxy species on acidic zeolite catalysts. *Acc Chem Res* 2008;41:895-904. DOI PubMed
42. Yamazaki H, Shima H, Imai H, Yokoi T, Tatsumi T, Kondo JN. Evidence for a "carbene-like" intermediate during the reaction of methoxy species with light alkenes on H-ZSM-5. *Angew Chem Int Ed Engl* 2011;50:1853-6. DOI PubMed
43. Yamazaki H, Shima H, Imai H, Yokoi T, Tatsumi T, Kondo JN. Direct production of propene from methoxy species and dimethyl ether over H-ZSM-5. *J Phys Chem C* 2012;116:24091-7. DOI
44. Minova IB, Bühl M, Matam SK, et al. Carbene-like reactivity of methoxy groups in a single crystal SAPO-34 MTO catalyst. *Catal Sci Technol* 2022;12:2289-305. DOI
45. Kubelková L, Nováková J, Jírů P. Reaction of small amounts of methanol on Hzsm-5, Hy and modified Y zeolites. Structure and Reactivity of Modified Zeolites, Proceedings of an International Conference. Elsevier; 1984. p. 217-24. DOI
46. Hutchings GJ, Gottschalk F, Hall MVM, Hunter R. Hydrocarbon formation from methylating agents over the zeolite catalyst ZSM-5. Comments on the mechanism of carbon-carbon bond and methane formation. *J Chem Soc., Faraday Trans* 1987;83:571-83. DOI
47. Tajima N, Tsuneda T, Toyama F, Hirao K. A new mechanism for the first carbon-carbon bond formation in the mtg process: a theoretical study. *J Am Chem Soc* 1998;120:8222-9. DOI
48. Liu Y, Kirchberger FM, Müller S, et al. Critical role of formaldehyde during methanol conversion to hydrocarbons. *Nat Commun* 2019;10:1462. DOI PubMed PMC
49. Wen W, Yu S, Zhou C, et al. Formation and fate of formaldehyde in methanol-to-hydrocarbon reaction: *in situ* synchrotron radiation photoionization mass spectrometry study. *Angew Chem Int Ed Engl* 2020;59:4873-8. DOI PubMed
50. Lesthaeghe D, Van Speybroeck V, Marin GB, Waroquier M. Understanding the failure of direct C-C coupling in the zeolite-catalyzed methanol-to-olefin process. *Angew Chem Int Ed Engl* 2006;45:1714-9. DOI PubMed
51. Dahl I, Kolboe S. On the reaction mechanism for hydrocarbon formation from methanol over SAPO-34: I. Isotopic labeling studies of the co-reaction of ethene and methanol. *J Catal* 1994;149:458-64. DOI
52. Dahl IM, Kolboe S. On the reaction mechanism for hydrocarbon formation from methanol over SAPO-34: 2. Isotopic labeling studies of the co-reaction of propene and methanol. *J Catal* 1996;161:304-9. DOI
53. Bjørgen M. The methanol-to-hydrocarbons reaction: insight into the reaction mechanism from [^{12}C]benzene and [^{13}C]methanol coreactions over zeolite H-beta. *J Catal* 2004;221:1-10. DOI
54. Svelle S, Joensen F, Nerlov J, et al. Conversion of methanol into hydrocarbons over zeolite H-ZSM-5: ethene formation is mechanistically separated from the formation of higher alkenes. *J Am Chem Soc* 2006;128:14770-1. DOI PubMed
55. Bjorgen M, Svelle S, Joensen F, et al. Conversion of methanol to hydrocarbons over zeolite H-ZSM-5: on the origin of the olefinic species. *J Catal* 2007;249:195-207. DOI
56. Van Speybroeck V, Van der Mynsbrugge J, Vandichel M, et al. First principle kinetic studies of zeolite-catalyzed methylation reactions. *J Am Chem Soc* 2011;133:888-99. DOI PubMed
57. Svelle S, Rønning PO, Kolboe S. Kinetic studies of zeolite-catalyzed methylation reactions1. Coreaction of [^{12}C]ethene and [^{13}C]methanol. *Journal of Catalysis* 2004;224:115-23. DOI
58. Svelle S, Ronning P, Olsbye U, Kolboe S. Kinetic studies of zeolite-catalyzed methylation reactions. Part 2. Co-reaction of [^{12}C]propene or [^{12}C]n-butene and [^{13}C]methanol. *J Catal* 2005;234:385-400. DOI PubMed
59. Hill IM, Hashimi SA, Bhan A. Kinetics and mechanism of olefin methylation reactions on zeolites. *J Catal* 2012;285:115-23. DOI
60. Hill IM, Hashimi SA, Bhan A. Corrigendum to "kinetics and mechanism of olefin methylation reactions over zeolites". *J Catal* 2012;291:155-7. DOI
61. Hill IM, Ng YS, Bhan A. Kinetics of butene isomer methylation with dimethyl ether over zeolite catalysts. *ACS Catal* 2012;2:1742-8. DOI
62. Nozik D, Bell AT. Role of Ga^{3+} Sites in Ethene Oligomerization over Ga/H-MFI. *ACS Catal* 2022;12:14173-84. DOI
63. Kim YT, Chada JP, Xu Z, et al. Low-temperature oligomerization of 1-butene with H-ferrierite. *J Catal* 2015;323:33-44. DOI
64. Dessau R. On the mechanism of methanol conversion to hydrocarbons over HZSM-5. *J Catal* 1982;78:136-41. DOI
65. Dessau R. On the H-ZSM-5 catalyzed formation of ethylene from methanol or higher olefins. *J Catal* 1986;99:111-6. DOI
66. Simonetti DA, Ahn JH, Iglesia E. Mechanistic details of acid-catalyzed reactions and their role in the selective synthesis of triptane and isobutane from dimethyl ether. *J Catal* 2011;277:173-95. DOI
67. Hay P, Redondo A, Guo Y. Theoretical studies of pentene cracking on zeolites: C-C β-scission processes. *Catal Today* 1999;50:517-23. DOI
68. Buchanan J, Santiesteban J, Haag W. Mechanistic considerations in acid-catalyzed cracking of olefins. *J Catal* 1996;158:279-87. DOI
69. Mikkelsen Ø, Kolboe S. The conversion of methanol to hydrocarbons over zeolite H-beta. *Microporous Mesoporous Mater* 1999;29:173-84. DOI

70. Teketel S, Skistad W, Benard S, et al. Shape selectivity in the conversion of methanol to hydrocarbons: the catalytic performance of one-dimensional 10-ring zeolites: ZSM-22, ZSM-23, ZSM-48, and EU-1. *ACS Catal* 2012;2:26-37. DOI
71. Yarulina I, Bailleul S, Pustovarenko A, et al. Suppression of the aromatic cycle in methanol-to-olefins reaction over ZSM-5 by post-synthetic modification using calcium. *ChemCatChem* 2016;8:3057-63. DOI
72. Martínez-espín JS, De Wispelaere K, Janssens TVW, et al. Hydrogen transfer versus methylation: on the genesis of aromatics formation in the methanol-to-hydrocarbons reaction over H-ZSM-5. *ACS Catal* 2017;7:5773-80. DOI
73. Arora SS, Bhan A. The critical role of methanol pressure in controlling its transfer dehydrogenation and the corresponding effect on propylene-to-ethylene ratio during methanol-to-hydrocarbons catalysis on H-ZSM-5. *J Catal* 2017;356:300-6. DOI
74. Fan S, Wang H, He S, et al. Formation and evolution of methylcyclohexene in the initial period of methanol to olefins over H-ZSM-5. *ACS Catal* 2022;12:12477-87. DOI
75. Lesthaeghe D, Horré A, Waroquier M, Marin GB, Van Speybroeck V. Theoretical insights on methylbenzene side-chain growth in ZSM-5 zeolites for methanol-to-olefin conversion. *Chemistry* 2009;15:10803-8. DOI PubMed
76. Xu T, Haw JF. Cyclopentenyl carbenium ion formation in acidic zeolites: an *in situ* NMR study of cyclic precursors. *J Am Chem Soc* 1994;116:7753-9. DOI
77. Haw JF, Nicholas JB, Song W, et al. Roles for cyclopentenyl cations in the synthesis of hydrocarbons from methanol on zeolite catalyst HZSM-5. *J Am Chem Soc* 2000;122:4763-75. DOI
78. Long J, Wang X, Ding Z, et al. Cyclopentadiene transformation over H-form zeolites: TPD and IR studies of the formation of a monomeric cyclopentenyl carbenium ion intermediate and its role in acid-catalyzed conversions. *J Catal* 2008;255:48-58. DOI
79. Wang C, Chu Y, Hu M, et al. Insight into carbocation-induced noncovalent interactions in the methanol-to-olefins reaction over ZSM-5 zeolite by solid-state NMR spectroscopy. *Angew Chem Int Ed Engl* 2021;60:26847-54. DOI PubMed
80. Arstad B, Nicholas JB, Haw JF. Theoretical study of the methylbenzene side-chain hydrocarbon pool mechanism in methanol to olefin catalysis. *J Am Chem Soc* 2004;126:2991-3001. DOI PubMed
81. Li J, Wei Y, Chen J, et al. Observation of heptamethylbenzenium cation over SAPO-type molecular sieve DNL-6 under real MTO conversion conditions. *J Am Chem Soc* 2012;134:836-9. DOI PubMed
82. Ilias S, Khare R, Malek A, Bhan A. A descriptor for the relative propagation of the aromatic- and olefin-based cycles in methanol-to-hydrocarbons conversion on H-ZSM-5. *J Catal* 2013;303:135-40. DOI
83. Sun X, Mueller S, Shi H, et al. On the impact of co-feeding aromatics and olefins for the methanol-to-olefins reaction on HZSM-5. *J Catal* 2014;314:21-31. DOI
84. Sun X, Mueller S, Liu Y, et al. On reaction pathways in the conversion of methanol to hydrocarbons on HZSM-5. *J Catal* 2014;317:185-97. DOI
85. Khare R, Arora SS, Bhan A. Implications of cofeeding acetaldehyde on ethene selectivity in methanol-to-hydrocarbons conversion on MFI and Its Mechanistic Interpretation. *ACS Catal* 2016;6:2314-31. DOI
86. Zhang C, Ng KLA, Yan L, et al. Kinetic Perspective on methanol to propylene process via HZSM-5 catalyst: balancing between reaction and diffusion. *Ind Eng Chem Res* 2022;61:2055-67. DOI
87. Goetze J, Meirer F, Yarulina I, et al. Insights into the activity and deactivation of the methanol-to-olefins process over different small-pore zeolites as studied with operando uv-vis spectroscopy. *ACS Catal* 2017;7:4033-46. DOI PubMed PMC
88. Borodina E, Meirer F, Lezcano-González I, et al. Influence of the reaction temperature on the nature of the active and deactivating species during methanol to olefins conversion over H-SSZ-13. *ACS Catal* 2015;5:992-1003. DOI
89. Borodina E, Sharbini Harun Kamaluddin H, Meirer F, et al. Influence of the reaction temperature on the nature of the active and deactivating species during methanol-to-olefins conversion over H-SAPO-34. *ACS Catal* 2017;7:5268-81. DOI PubMed PMC
90. Qi L, Li J, Wei Y, Xu L, Liu Z. Role of naphthalene during the induction period of methanol conversion on HZSM-5 zeolite. *Catal Sci Technol* 2016;6:3737-44. DOI
91. Yarulina I, Goetze J, Gücüyener C, et al. Methanol-to-olefins process over zeolite catalysts with DDR topology: effect of composition and structural defects on catalytic performance. *Catal Sci Technol* 2016;6:2663-78. DOI
92. Teketel S, Svelle S, Lillerud K, Olsbye U. Shape-selective conversion of methanol to hydrocarbons over 10-ring unidirectional-channel acidic H-ZSM-22. *ChemCatChem* 2009;1:78-81. DOI
93. Teketel S, Olsbye U, Lillerud K, Beato P, Svelle S. Selectivity control through fundamental mechanistic insight in the conversion of methanol to hydrocarbons over zeolites. *Microporous Mesoporous Mater* 2010;136:33-41. DOI
94. Cnudde P, Demuynck R, Vandenbrande S, Waroquier M, Sastre G, Speybroeck VV. Light olefin diffusion during the MTO process on H-SAPO-34: a complex interplay of molecular factors. *J Am Chem Soc* 2020;142:6007-17. DOI PubMed
95. Crank J. The mathematics of diffusion. 2nd edition. Oxford University Press; 1979. DOI
96. Koller H, Kärger J, Ruthven DM. Theodorou DN. Sorption kinetics. In “Diffusion in nanoporous materials”. Wiley-VCH: Weinheim; 2012. p. 1433-7851. DOI
97. Khare R, Millar D, Bhan A. A mechanistic basis for the effects of crystallite size on light olefin selectivity in methanol-to-hydrocarbons conversion on MFI. *J Catal* 2015;321:23-31. DOI
98. Khare R, Bhan A. Mechanistic studies of methanol-to-hydrocarbons conversion on diffusion-free MFI samples. *J Catal* 2015;329:218-28. DOI
99. Liu Z, Dong X, Zhu Y, et al. Investigating the influence of mesoporosity in zeolite beta on its catalytic performance for the conversion of methanol to hydrocarbons. *ACS Catal* 2015;5:5837-45. DOI

100. Wei R, Li C, Yang C, Shan H. Effects of ammonium exchange and Si/Al ratio on the conversion of methanol to propylene over a novel and large partical size ZSM-5. *J Nat Gas Chem* 2011;20:261-5. DOI
101. Zhao X, Wang L, Li J, et al. Investigation of methanol conversion over high-Si beta zeolites and the reaction mechanism of their high propene selectivity. *Catal Sci Technol* 2017;7:5882-92. DOI
102. Yarulina I, De Wispelaere K, Bailleul S, et al. Structure-performance descriptors and the role of Lewis acidity in the methanol-to-propylene process. *Nat Chem* 2018;10:804-12. DOI PubMed
103. Khare R, Liu Z, Han Y, Bhan A. A mechanistic basis for the effect of aluminum content on ethene selectivity in methanol-to-hydrocarbons conversion on HZSM-5. *J Catal* 2017;348:300-5. DOI
104. Liang T, Chen J, Qin Z, et al. Insight into induction period of methanol conversion reaction: reactivity of ethene-precursors over H-ZSM-5 zeolite is independent of Brϕnsted acid site density. *Fuel* 2023;332:126062. DOI
105. Yuan K, Jia X, Wang S, et al. Regulating the distribution of acid sites in ZSM-11 zeolite with different halogen anions to enhance its catalytic performance in the conversion of methanol to olefins. *MicroporousMesoporous Mater* 2022;341:112051. DOI
106. Hereijgers BP, Bleken F, Nilsen MH, et al. Product shape selectivity dominates the methanol-to-olefins (MTO) reaction over H-SAPO-34 catalysts. *J Catal* 2009;264:77-87. DOI
107. Kang JH, Alshafei FH, Zones SI, Davis ME. Cage-defining ring: a molecular sieve structural indicator for light olefin product distribution from the methanol-to-olefins reaction. *ACS Catal* 2019;9:6012-9. DOI
108. Hwang A, Prieto-centurion D, Bhan A. Isotopic tracer studies of methanol-to-olefins conversion over HSAPO-34: the role of the olefins-based catalytic cycle. *J Catal* 2016;337:52-6. DOI
109. Hua J, Dong X, Wang J, et al. Methanol-to-olefin conversion over small-pore ddr zeolites: tuning the propylene selectivity via the olefin-based catalytic cycle. *ACS Catal* 2020;10:3009-17. DOI
110. Yang M, Li B, Gao M, et al. High Propylene selectivity in methanol conversion over a small-pore SAPO molecular sieve with ultra-small cage. *ACS Catal* 2020;10:3741-9. DOI
111. Zhou Y, Zhang J, Ma W, et al. Small pore SAPO-14-based zeolites with improved propylene selectivity in the methanol to olefins process. *Inorg Chem Front* 2022;9:1752-60. DOI
112. Dyballa M, Becker P, Trefz D, et al. Parameters influencing the selectivity to propene in the MTO conversion on 10-ring zeolites: directly synthesized zeolites ZSM-5, ZSM-11, and ZSM-22. *AAPPL CATAL A-GEN* 2016;510:233-43. DOI
113. Lee K, Lee H, Ihm S. Influence of catalyst binders on the acidity and catalytic performance of HZSM-5 zeolites for methanol-to-propylene (MTP) process: single and binary binder system. *Top Catal* 2010;53:247-53. DOI
114. Hu Z, Zhang H, Wang L, et al. Highly stable boron-modified hierarchical nanocrystalline ZSM-5 zeolite for the methanol to propylene reaction. *Catal Sci Technol* 2014;4:2891-5. DOI
115. Yoshioka M, Yokoi T, Tatsumi T. Development of the CON-type aluminosilicate zeolite and its catalytic application for the MTO reaction. *ACS Catal* 2015;5:4268-75. DOI
116. Zhao X, Wang L, Guo P, et al. Synthesis of high-Si hierarchical beta zeolites without mesoporogen and their catalytic application in the methanol to propene reaction. *Catal Sci Technol* 2018;8:2966-74. DOI
117. Jamil AK, Muraza O, Yoshioka M, Al-amer AM, Yamani ZH, Yokoi T. Selective production of propylene from methanol conversion over nanosized ZSM-22 zeolites. *Ind Eng Chem Res* 2014;53:19498-505. DOI
118. Zhang J, Huang Z, Li P, et al. Elucidating the reaction pathway for ethene and propene formation in the methanol-to-hydrocarbons reaction over high silica H-Beta. *Catal Sci Technol* 2017;7:2194-203. DOI
119. Wennmacher JTC, Mahmoudi S, Rzepka P, et al. Electron diffraction enables the mapping of coke in ZSM-5 micropores formed during methanol-to-hydrocarbons conversion. *Angew Chem Int Ed Engl* 2022;61:e202205413. DOI PubMed PMC
120. Schmidt F, Hoffmann C, Giordanino F, et al. Coke location in microporous and hierarchical ZSM-5 and the impact on the MTH reaction. *J Catal* 2013;307:238-45. DOI
121. Urata K, Furukawa S, Komatsu T. Location of coke on H-ZSM-5 zeolite formed in the cracking of n-hexane. *AAPPL CATAL A-GEN* 2014;475:335-40. DOI
122. Milina M, Mitchell S, Cooke D, Crivelli P, Pérez-Ramírez J. Impact of pore connectivity on the design of long-lived zeolite catalysts. *Angew Chem Int Ed Engl* 2015;54:1591-4. DOI PubMed
123. Astafan A, Benghalem M, Pouilloux Y, et al. Particular properties of the coke formed on nano-sponge *BEA zeolite during ethanol-to-hydrocarbons transformation. *J Catal* 2016;336:1-10. DOI
124. Müller S, Liu Y, Vishnuvarthan M, et al. Coke formation and deactivation pathways on H-ZSM-5 in the conversion of methanol to olefins. *Journal of Catalysis* 2015;325:48-59. DOI
125. Lezcano-Gonzalez I, Campbell E, Hoffman AEJ, et al. Insight into the effects of confined hydrocarbon species on the lifetime of methanol conversion catalysts. *Nat Mater* 2020;19:1081-7. DOI PubMed
126. Bjørgen M. Coke precursor formation and zeolite deactivation: mechanistic insights from hexamethylbenzene conversion. *J Catal* 2003;215:30-44. DOI
127. Magnoux P, Roger P, Canaff C, Fouche V, Gnep N, Guisnet M. New technique for the characterization of carbonaceous compounds responsible for zeolite deactivation. Catalyst Deactivation 1987, Proceedings of the 4th International Symposium. Elsevier; 1987. p. 317-30. DOI
128. Aramburo LR, Teketel S, Svelle S, et al. Interplay between nanoscale reactivity and bulk performance of H-ZSM-5 catalysts during the methanol-to-hydrocarbons reaction. *J Catal* 2013;307:185-93. DOI

129. Wei Y, Yuan C, Li J, et al. Coke formation and carbon atom economy of methanol-to-olefins reaction. *ChemSusChem* 2012;5:906-12. DOI PubMed
130. Wragg DS, O'Brien MG, Bleken FL, Di Michiel M, Olsbye U, Fjellvåg H. Watching the methanol-to-olefin process with time- and space-resolved high-energy operando X-ray diffraction. *Angew Chem Int Ed Engl* 2012;51:7956-9. DOI PubMed
131. Wang C, Wang Q, Xu J, et al. Direct detection of supramolecular reaction centers in the methanol-to-olefins conversion over zeolite H-ZSM-5 by ^{13}C-^{27}Al solid-state NMR spectroscopy. *Angew Chem Int Ed Engl* 2016;55:2507-11. DOI
132. Yang L, Wang C, Zhang L, et al. Stabilizing the framework of SAPO-34 zeolite toward long-term methanol-to-olefins conversion. *Nat Commun* 2021;12:4661. DOI PubMed PMC
133. Wang N, Zhi Y, Wei Y, et al. Molecular elucidating of an unusual growth mechanism for polycyclic aromatic hydrocarbons in confined space. *Nat Commun* 2020;11:1079. DOI PubMed PMC
134. Wang C, Yang M, Tian P, et al. Dual template-directed synthesis of SAPO-34 nanosheet assemblies with improved stability in the methanol to olefins reaction. *J Mater Chem A* 2015;3:5608-16. DOI
135. Choi M, Na K, Kim J, Sakamoto Y, Terasaki O, Ryoo R. Stable single-unit-cell nanosheets of zeolite MFI as active and long-lived catalysts. *Nature* 2009;461:246-9. DOI PubMed
136. Liu Y, Zhang Q, Li J, et al. Protozeolite-seeded synthesis of single-crystalline hierarchical zeolites with facet-shaped mesopores and their catalytic application in methanol-to-propylene conversion. *Angew Chem Int Ed Engl* 2022;61:e202205716. DOI PubMed
137. Liang T, Chen J, Wang S, et al. Conversion of methanol to hydrocarbons over H-MCM-22 zeolite: deactivation behaviours related to acid density and distribution. *Catal Sci Technol* 2022;12:6268-84. DOI
138. Liu Z, Dong X, Liu X, Han Y. Oxygen-containing coke species in zeolite-catalyzed conversion of methanol to hydrocarbons. *Catal Sci Technol* 2016;6:8157-65. DOI
139. Chen Z, Ni Y, Zhi Y, et al. Coupling of methanol and carbon monoxide over H-ZSM-5 to form aromatics. *Angew Chem Int Ed Engl* 2018;57:12549-53. DOI PubMed
140. Shi Z, Arora SS, Trahan DW, Hickman D, Bhan A. Methanol to hydrocarbons conversion: Why dienes and monoenes contribute differently to catalyst deactivation? *Chem Eng J* 2022;437:134229. DOI
141. Martinez-espin JS, Mortén M, Janssens TVW, Svelle S, Beato P, Olsbye U. New insights into catalyst deactivation and product distribution of zeolites in the methanol-to-hydrocarbons (MTH) reaction with methanol and dimethyl ether feeds. *Catal Sci Technol* 2017;7:2700-16. DOI
142. Shi Z, Neurock M, Bhan A. Methanol-to-olefins catalysis on HSSZ-13 and HSAPO-34 and Its relationship to acid strength. *ACS Catal* 2021;11:1222-32. DOI
143. Hwang A, Bhan A. Bifunctional strategy coupling Y_2O_3-catalyzed alkanal decomposition with methanol-to-olefins catalysis for enhanced lifetime. *ACS Catal* 2017;7:4417-22. DOI
144. Arora SS, Nieskens DLS, Malek A, Bhan A. Lifetime improvement in methanol-to-olefins catalysis over chabazite materials by high-pressure H_2 co-feeds. *Nat Catal* 2018;1:666-72. DOI
145. Hwang A, Bhan A. Deactivation of zeolites and zeotypes in methanol-to-hydrocarbons catalysis: mechanisms and circumvention. *Acc Chem Res* 2019;52:2647-56. DOI PubMed
146. Zhou J, Gao M, Zhang J, et al. Directed transforming of coke to active intermediates in methanol-to-olefins catalyst to boost light olefins selectivity. *Nat Commun* 2021;12:17. DOI PubMed PMC
147. Wang C, Yang L, Gao M, et al. Directional construction of active naphthalenic species within SAPO-34 crystals toward more efficient methanol-to-olefin conversion. *J Am Chem Soc* 2022;144:21408-16. DOI PubMed
148. Gao P, Wang Q, Xu J, et al. Brønsted/lewis acid synergy in methanol-to-aromatics conversion on ga-modified zsm-5 zeolites, as studied by solid-state NMR spectroscopy. *ACS Catal* 2018;8:69-74. DOI
149. Wang N, Li J, Sun W, et al. Rational design of zinc/zeolite catalyst: selective formation of p-Xylene from methanol to aromatics reaction. *Angew Chem Int Ed Engl* 2022;61:e202114786. DOI PubMed
150. Wang H, Wang L, Luo Q, et al. Two-dimensional manganese oxide on ceria for the catalytic partial oxidation of hydrocarbons. *Chem Synth* 2022;2:2. DOI
151. Wang D, Xie Z, Porosoff MD, Chen JG. Recent advances in carbon dioxide hydrogenation to produce olefins and aromatics. *Chem* 2021;7:2277-311. DOI
152. Zhang W, Wang S, Guo S, et al. Effective conversion of CO_2 into light olefins over a bifunctional catalyst consisting of La-modified ZnZrO. *Catal Sci Technol* ;12:2566-77. DOI
153. Xie J, Firth DS, Cordero-Lanzac T, et al. MAPO-18 catalysts for the methanol to olefins process: influence of catalyst acidity in a high-pressure syngas (CO and H_2) environment. *ACS Catal* 2022;12:1520-31. DOI PubMed PMC
154. Wang S, Zhang L, Wang P, et al. Highly selective hydrogenation of CO_2 to propane over $GaZrO_x$/H-SSZ-13 composite. *Nat Catal* 2022;5:1038-50. DOI